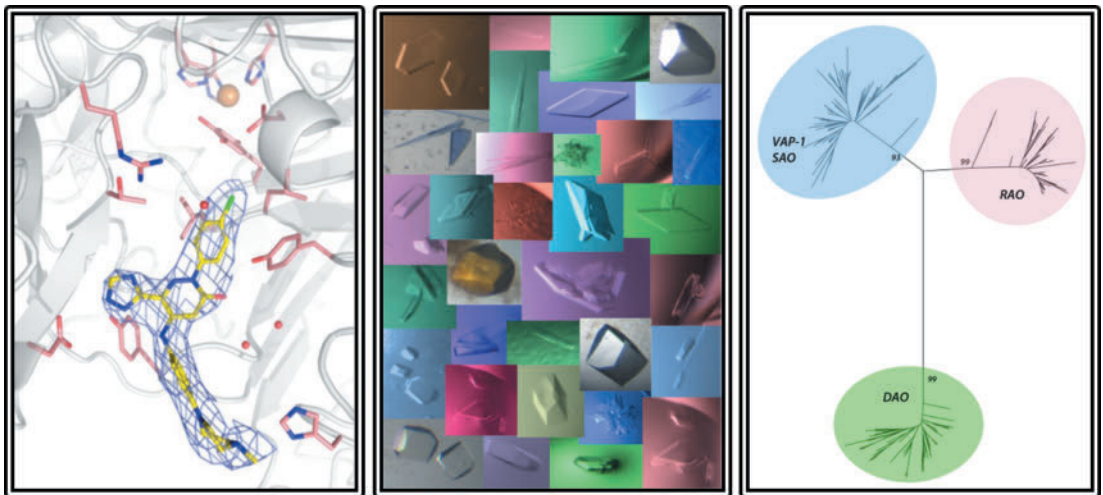Eva Bligt-Lindén

VAP-1 as drug target in inflammation:

Structural features determining ligand interactions

Eva Bligt-Lindén

was born on October 10, 1984 in Vaasa, Finland. She graduated from Åbo Akademi University in 2009 with a Master of Science in Bioscience. This PhD thesis project in Biochemistry has taken place during 2010-2015 under the supervision of Docent Tiina A. Salminen at the Faculty of Science and Engineering.

VAP-1 as drug target in inflammation: Structural features determining ligand interactions

Eva Bligt-Lindén

Biochemistry, Faculty of Science and Engineering
Åbo Akademi University
Turku, Finland
2015

From the Faculty of Science and Engineering, Åbo Akademi University & National Doctoral Programme in Informational and Structural Biology

Supervised by:

Docent Tiina A. Salminen, PhD
Faculty of Science and Engineering
Åbo Akademi University
Turku, Finland

Reviewed by:

Professor Juha Rouvinen, PhD
Department of Chemistry
University of Eastern Finland
Joensuu, Finland

and

Academy of Finland Research Fellow Lari Lehtiö, PhD
Faculty of Biochemistry and Molecular Medicine
University of Oulu
Oulu, Finland

Opponent:

Assistant Professor Maria Luisa Di Paolo, PhD
Department of Molecular Medicine
University of Padova
Padova, Italy

Cover, from left: Electron density map of pyridazinone inhibitor 13 bound to human VAP-1, figure adapted from publication I. Protein crystals produced and photographed by Dr. Lesa Offermann. Phylogenetic tree of the copper amine oxidases, figure made by Leonor Lopes de Carvalho.

Somewhere, something incredible is waiting to be known.

-Carl Sagan

TABLE OF CONTENTS

ABSTRACT

Vascular adhesion protein-1 (VAP-1), which belongs to the copper amine oxidases (CAOs), is a validated drug target in inflammatory diseases. Inhibition of VAP-1 blocks the leukocyte trafficking to sites of inflammation and alleviates inflammatory reactions. In this study, a novel set of potent pyridazinone inhibitors is presented together with their X-ray structure complexes with VAP-1. The crystal structure of serum VAP-1 (sVAP-1) revealed an imidazole binding site in the active site channel and, analogously, the pyridazinone inhibitors were designed to bind into the channel. This is the first time human VAP-1 has been crystallized with a reversible inhibitor and the structures reveal detailed information of the binding mode on the atomic level.

Similarly to some earlier studied inhibitors of human VAP-1, the designed pyridazinone inhibitors bind rodent VAP-1 with a lower affinity than human VAP-1. Therefore, we made homology models of rodent VAP-1 and compared human and rodent enzymes to determine differences that might affect the inhibitor binding. The comparison of the crystal structures of the human VAP-1 and the mouse VAP-1 homology model revealed key differences important for the species specific binding properties. In general, the channel in mouse VAP-1 is more narrow and polar than the channel in human VAP-1, which is wider and more hydrophobic. The differences are located in the channel leading to the active site, as well as, in the entrance to the active site channel. The information obtained from these studies is of great importance for the development and design of drugs blocking the activity of human VAP-1, as rodents are often used for *in vivo* testing of candidate drugs.

In order to gain more insight into the selective binding properties of the different CAOs in one species a comprehensive evolutionary study of mammalian CAOs was performed. We found that CAOs can be classified into sub-families according to the residues X1 and X2 of the Thr/Ser-X1-X2-Asn-Tyr-Asp active site motif. In the phylogenetic tree, CAOs group into diamine oxidase, retina specific amine oxidase and VAP-1/serum amine oxidase clades based on the

residue in the position X2. We also found that VAP-1 and SAO can be further differentiated based on the residue in the position X1. This is the first large-scale comparison of CAO sequences, which explains some of the reasons for the unique substrate specificities within the CAO family.

SAMMANFATTNING

Vaskulärt adhesionsprotein-1 (VAP-1) tillhör enzymfamiljen kopparhaltiga aminoxidaser (CAO). VAP-1 är involverat i leukocyternas inträde i endotelceller vid inflammation och inhibition av dess funktion har en bevisad antiinflammatorisk verkan. I denna studie presenteras nya typer av VAP-1-pyridazinoninhibitorer. Inhibitorerna är designade att binda till det sekundära imidazolbindningsstället i kanalen som leder fram till det aktiva stället hos VAP-1. Det sekundära imidazolbindningsstället identifierades i samband med strukturbestämningen av serumVAP-1. Detta är den första gången VAP-1 har samkristalliserats med en reversibel inhibitor. Den tredimensionella strukturen beskriver proteinets och inhibitorernas interaktioner på atomnivå.

Trots att dessa inhibitorer uppvisar potent och specifik bindning till humant VAP-1 så binder de musens VAP-1 med lägre affinitet. Genom sekvensjämförelser och jämförelse av musens VAP-1-homologimodell med kristallstrukturen av humant VAP-1 kunde artspecifika aminosyraskillnader som orsakar den sämre bindningen hos musens VAP-1 identifieras. Dessa skillnader finns i kanalen som leder till det aktiva stället, samt vid ingången till kanalen. Kanalen som leder till det aktiva stället är bredare och mera hydrofob i humant VAP-1 än kanalen i musens VAP-1, som är smalare och mera polär. Dessa resultat är viktiga vid utvecklingen av nya typspecifika läkemedel mot människans VAP-1 eftersom gnagare ofta används för *in vivo*-testande av läkemedel.

Hittills har klassificeringen av de olika CAO-familjemedlemmarna varit bristfällig och felaktiga annoteringar har förekommit. I vår evolutionära undersökning av de olika CAO-familjemedlemmarna hos däggdjur kunde vi fastställa ett klassificeringssätt baserat på aminosyrorna X1 och X2 i motivet för det aktiva stället: Thr/Ser-X1-X2-Asn-Tyr-Asp. Diaminoxidas, retina-specifikt aminoxidas och VAP-1/serumaminoxidas grupperar sig i olika grenar i det fylogenetiska trädet baserat på aminosyran i position X2. VAP-1 och serumaminoxidas kan ytterligare skiljas åt baserat på aminosyran i position X1.

Detta är den första omfattande evolutionära studien av CAO. Dessa kriterier underlättar en korrekt klassificering av det snabbt ökande antalet nyidentifierade CAOs och resultaten är viktiga vid designen av typspecifika inhibitorer för de olika CAO-familjemedlemmarna.

LIST OF ORIGINAL PUBLICATIONS

This thesis is based on the following original publications, which are referred to by Roman numerals (I-IV) in the text. Publications and figures are reprinted with permission from the publishers.

I.   Heli Elovaara*, Heidi Kidron*, Vimal Parkash*, Yvonne Nymalm, **Eva Bligt**, Pauli Ollikka, David J. Smith, Marjo Pihlavisto, Marko Salmi, Sirpa Jalkanen and Tiina A. Salminen. (2011) Identification of two imidazole binding sites and key residues for substrate specificity in human serum primary amine oxidase. *Biochemistry, 50: 5507–5520* (*equal contribution)

II.   **Eva Bligt-Lindén**, Marjo Pihlavisto, István Szatmári, Zbyszek Otwinowski, David J. Smith, László Lázár, Ferenc Fülöp and Tiina A. Salminen. (2013) Novel pyridazinone inhibitors for vascular adhesion protein-1 (VAP-1): old target-new inhibition mode. *Journal of Medicinal Chemistry 56: 9837-9848*

III. **Eva Bligt-Lindén**, Ramaiah Arunachalam, Vimal Parkash and Tiina A. Salminen. (2013) Structural comparison of the active site channels in rodent and primate vascular adhesion protein-1. *Journal of Neural Transmission 120: 947-950*

IV.   Leonor Lopes de Carvalho, **Eva Bligt-Lindén**, Ramaiah Arunachalam, Mark S. Johnson and Tiina A. Salminen (2015) Evolution and functional classification of mammalian copper-containing amine oxidases. *Manuscript*

CONTRIBUTIONS OF THE AUTHOR

The work was designed and manuscripts were written together with the supervisor. All co-authors contributed to the final manuscripts. Publications II and III were mainly written by the author.

I. The author participated in the refinement, validation and visualization of the crystal structures. The author participated in the editing of the text and pictures in the manuscript.

II. All the X-ray crystallographic studies, including crystallization, data collection, structure solution, refinement and structure validation, were performed by the author. Dr. Zbyszek Otwinowski assisted in the diffraction data processing. The author also performed the homology modeling.

III. The sequence alignments, homology modeling and structural comparisons were done by the author.

IV. The author participated in the planning of the work, the analysis of the results and the writing of the paper together with the supervisor. PhD student Leonor Lopes de Carvalho performed the study and was mainly responsible for writing the manuscript.

Additional publications not included in the thesis

Kristiina Aalto, Anu Autio, Elina Kivi, Kati Elima, Yvonne Nymalm, Heli Elovaara, Tiina Saanijoki, Paul R. Crocker, Mikael Maksimow, **Eva Bligt**, Tiina A. Salminen, Marko Salmi, Anne Roivainen and Sirpa Jalkanen. (2011) Siglec-9 is a novel leukocyte ligand for Vascular Adhesion Protein-1 (VAP-1) and can be utilized in PET-imaging of cancer and inflammation. *Blood, 118: 3725-3733*

Matti Lahti*, **Eva Bligt***, Henri Niskanen, Anna Brandt, Vimal Parkash, Johanna Jokinen, Pekka Patrikainen, Jarmo Käpylä, Jyrki Heino and Tiina Salminen. (2011) Structure of the collagen receptor integrin alpha1I domain carrying the activating mutation E317A. *Journal of Biological Chemistry 50: 43343-51* (* equal contribution)

ACKNOWLEDGEMENTS

Singh Chouhan, Stina Sandberg and Outi Salo-Ahen. Käthe, I am glad that we crossed paths in SBL. You have been a tremendous support for me during these years and for that I am deeply grateful. You have been an excellent travel companion to courses and conferences. I have appreciated all of our scientific and non-scientific discussions. In addition, you have been a superb playmate for Edvin. Thank you Lenita, Yvonne and Anna for welcoming me into SBL. I appreciate your patience and all the practical help I got during my start in the lab. I would like to thank Vimal and Leonor for nice collaboration and co-authorship. I would like to thank Jukka for managing and solving every computer related problem that I have encountered during my stay at SBL. Santtu, Tomi, Bhanu, Stina and Outi, I appreciate all discussions we have had during the years.

I like to acknowledge the people in the former Biochemistry department. I want to thank *Elsmarie Nyman, Pirkko Luoma, Eve Hed-Kattelus, Jussi Meriluoto* and *Juha-Pekka Sunila* for all administrative and technical help I have received during the years at the department. I also want to extend my gratitude to my fellow graduate students inside and outside BioCity. *Gloria, Daniela* and *Marika*, it has been a pleasure to share this journey with you. I am proud not only to call you my colleagues but also my friends. I have appreciated all our discussions and I want to thank you for helping me in my work through your knowledge in doing research.

My dear friends, I am glad to have you all in my life. You encourage me in my work and in my life. *Ninni, Heidi, Ida* and *Gunilla*, we shared great moments during the masters studies, then you escaped BioCity but we stayed in touch and we have shared many great times during these years. Hopefully, there are many more to come. *Pia, Carro, Leena, Tette* and *Sandra*, I thank you for your friendship and support. You keep me aware about the world outside of science. I really enjoy our laughter and endless discussions just about anything and everything.

I want to thank my family for their endless support. My parents, *Rose-Marie* and *Anders*, are a continuous support and I want to thank them for all their help. My

brothers, *Mikael* and *Roy*, you are important to me and I am grateful that I can depend on you in times of need. At last, my greatest appreciation goes to my dear husband, *Isak*. Thank you for all our years together, for your love and support. Finally, I want to thank our son, *Edvin*, for keeping me on my toes and for all the love we share.

Eva Bligt-Lindén

Jeppo, November 2015

ABBREVIATIONS

2HP	2-hydrazinopyridine
bSAO	Bovine serum amine oxidase
CAO	Copper amine oxidase
CHO	Chinese hamster ovary cell lines
DAO	Diamine oxidase
FAD	Flavin adenine dinucleotide
HEK	Hamster embryonic kidney cells
hVAP-1	Human vascular adhesion protein-1
IC_{50}	Mean inhibitory concentration
JTT	Jones-Taylor-Thornton substitution matrix
K_a	Association constant
K_d	Dissociation constant
LTQ	Lysine tyrosylquinone
MAO	Mono amine oxidase
ML	Maximum likelihood method
NJ	Neighbor-Joining method
PDB	Protein data bank
PET	Positron emission tomography
PO	Polyamine oxidase
RAO	Retina specific amine oxidase
Rmsd	Root-mean-square deviation
SAO	Serum amine oxidase
sVAP-1	Serum vascular adhesion protein-1
TPQ	2,4,5-trihydroxyphenylalanine quinone
VAP-1	Vascular adhesion protein-1

1. INTRODUCTION

There is an increasing need for anti-inflammatory therapy since a major part of contemporary human diseases in the Western countries is of an inflammatory nature. Vascular adhesion protein-1 (VAP-1) is a primary copper amine oxidase (CAO) and cell adhesion receptor, which is involved in several pathological conditions due to its proinflammatory effects and involvement in the leukocyte trafficking to sites of inflammation (Salmi & Jalkanen, 2014). Human VAP-1 has great potential as a drug target in acute and chronic inflammatory conditions like rheumatoid arthritis, psoriasis, atopic eczema, multiple sclerosis, diabetes, and respiratory diseases (Dunkel et al., 2011). There are two major strategies used to inhibit VAP-1; small molecular inhibitors and antibodies (Dunkel et al., 2011). The majority of the small molecular inhibitors are targeted to the active site cofactor of VAP-1. However, this irreversible mode of inhibition, where new enzyme synthesis is required to recover enzyme activity (Palfreyman et al., 1994), is an undesirable characteristic for a drug for human use. The ability to remove a drug and regain target activity within a short period of time is important and the active site channel of VAP-1 presents an advantageous alternative binding site for reversibly binding inhibitors in relation to the active site cofactor. In order to effectively develop inhibitors to target VAP-1, it is critical to understand the function of the protein on a cellular level, as well as, on a molecular level. In this study, a novel set of inhibitors and their binding mode to VAP-1 were evaluated with X-ray crystallography. Computational and experimental studies, together with evolutionary studies, further increase the knowledge about the protein function and the CAO family, which is of importance in the design of specific and potent inhibitors.

2. REVIEW OF THE LITERATURE

2.1 Amine oxidases

Amine oxidases are a family of proteins, which oxidize amines to their corresponding aldehydes in a reaction where hydrogen peroxide and ammonia are produced. The family consists of monoamine oxidases (MAO, EC 1.4.3.4), polyamine oxidases (PO, EC 1.5.3.17) and the copper amine oxidases (Floris, 2009). MAOs and POs have flavin adenine dinucleotide (FAD) as cofactor, while the copper amine oxidases can be further classified based on their quinone cofactor (Klinman, 1996), which is either a 2,4,5-trihydroxyphenylalanine quinone (TPQ) in copper-containing amine oxidases (CAOs; EC 1.4.3.21 primary amine oxidase and EC 1.4.2.22 diamine oxidase) or a lysine tyrosyl-quinone (LTQ) in lysyl oxidases (LOXs, EC. 1.4.3.13) (Klinman, 1996).

Two isoforms of MAO are present in humans: MAO A and MAO B. Both are located in the outer mitochondrial membrane of mammalian cells, and they catalyze the deamination of primary, secondary and tertiary amines. MAOs are linked to depression (Meyer et al., 2006) and they metabolize neurotransmitters such as serotonin, norepinephrine and dopamine (Shih et al., 1999). There are three isoforms of the POs and they are involved in the regulation of cellular growth by oxidizing polyamines such as spermine and spermidine (Seiler, 2004), while the CAOs oxidize primary amines. The members of the LOX family can convert the amino group of a lysine to an aldehyde and the product aldehyde can then react with a second lysine-derived aldehyde to form crosslinks important in the formation and stabilization of collagen and elastin (Lucero & Kagan, 2006).

2.2 CAOs

There are four genes, *AOC1-4*, coding for CAOs in mammals (Schwelberger, 2007). *AOC1* encodes diamine oxidase (DAO) (EC 1.4.3.22), *AOC2* encodes retina specific amine oxidase (RAO), *AOC3* encodes vascular adhesion protein-1 (VAP-1) (EC 1.4.3.21), and *AOC4* encodes a soluble paralog of VAP-1 called serum amine oxidase (SAO). All four genes have been identified in humans, pigs, horses, dogs, mice, rats, chimpanzees and macaques (Schwelberger, 2007). However, the *AOC4* gene in human and the *AOC2* gene in rat contains one internal stop codon each, resulting in truncated and nonfunctional proteins (Schwelberger, 2007; Zhang et al., 2003). Rodents are also missing an *AOC4* gene

product as they only have small fragments of the *AOC4* gene (Schwelberger, 2007). The human AOC1 and AOC2/AOC3 share 38% sequence identity, AOC2 shares 65% identity with AOC3, while AOC3 and AOC4 share 90% identity. The interspecies sequence identity of mammalian CAOs (cow, horse, dog, chimpanzee, macaque, and human) is 80-95% (Schwelberger, 2010). The proteins are sometimes named AOC1, AOC2, AOC3 and AOC4, but in this thesis they are hereafter referred to as DAO, RAO, VAP-1 and SAO, respectively. The members of the CAO family all share a similar fold (Floris, 2009), which is discussed in chapter 2.4 where the structure of VAP-1 is presented in detail.

2.2.1 DAO (the *AOC1* gene product)

DAO is mainly expressed in the kidney, placenta, intestine and seminal vesicles (Elmore et al., 2002). The protein is released from the cells in response to an external stimulus and it oxidizes both endogenous and exogenous histamine (Schwelberger, 2007). DAO differs from the rest of the CAOs as it oxidizes diamines compared to the other proteins that oxidize monoamines (Elmore et al., 2002). A decrease in DAO activity correlates with histamine intolerance (Maintz & Novak, 2007) and the balance between DAO and histamine is important in achieving an uncomplicated pregnancy (Maintz et al., 2008). The structure of human DAO (hDAO) was determined by McGrath and coworkers in 2009 (McGrath et al., 2009).

2.2.2 RAO (the *AOC2* gene product)

RAO is the least known member of the CAOs. RAO was cloned from the retina of human in 1997 (Imamura et al., 1997). mRNA of RAO has been detected in the lung, brain, kidney, cartilage, tonsil and in the heart, but RAO activity has only been detected in the retina (Kaitaniemi et al., 2009). RAO oxidizes 2-phenylethylamine, tryptamine and p-tyramine *in vitro* (Kaitaniemi et al., 2009). The structure of RAO is not known but a structural model has been made based on the X-ray structure of human VAP-1(Kaitaniemi et al., 2009). The overall fold of RAO is likely to be similar to the fold of hVAP-1 because of their high sequence identity (68%).

2.2.3 VAP-1 (the *AOC3* gene product)

VAP-1 was cloned in 1998 (Smith et al., 1998) and it is expressed in adipocytes, vascular endothelial cells and in smooth muscle cells (Salmi & Jalkanen, 1992;

Salmi & Jalkanen, 2001; Zorzano et al., 2003). In endothelial cells VAP-1 is stored within intracellular granules, and upon inflammatory stimuli it is rapidly translocated to the cell surface (Jaakkola et al., 2000; Salmi et al., 1997; Vainio et al., 2005). Preferred substrates for VAP-1 are soluble amines like methylamine and aminoacetone, which are formed during intermediary metabolism (Lyles & Chalmers, 1992). VAP-1 is involved in several diseases and pathophysiological conditions, which will be discussed later in the text (Boomsma et al., 2003). VAP-1 is primarily a membrane-bound extracellular protein but it can also be proteolytically cleaved and exists in a soluble form in the blood (referred to as serum VAP-1 (sVAP-1)) (Abella et al., 2004; Kurkijarvi et al., 1998; Stolen et al., 2005). As humans are lacking SAO, it is the cleaved sVAP-1 that gives rise to the VAP-1 activity in the blood.

2.2.4 SAO (the *AOC4* gene product)

Mature SAO results from the cleavage of a signal peptide, leaving the protein soluble in contrast to the membrane-bound RAO and VAP-1, which have an N-terminal transmembrane helix. In contrast to human, which is missing functional SAO, mammals such as cow, horse, pig and sheep have high levels of SAO activity in their blood (Boomsma et al., 2003; Schwelberger, 2007). Bovine SAO (bSAO) shows high affinity for physiological polyamines such as spermine, spermidine, long hydrophobic amines and benzylamine with hydrophobic substituents (Buffoni, 1966; Di Paolo et al., 2003; Hartmann & Klinman, 1991). The crystal structure of bSAO was determined by Lunelli and coworkers in 2005 (Lunelli et al., 2005).

2.3 The TPQ cofactor and the reaction mechanism of CAOs

The CAO cofactor TPQ is derived from a post-translationally modified tyrosine within the active site of the protein. Two possible conformations of the TPQ have been detected in the X-ray structures (Figure 1) (Parsons et al., 1995). It can adopt an on-copper conformation (Figure 1A), which is the inactive or resting conformation, and an active off-copper conformation (Figure 1B). In the inactive conformation, the O4 of TPQ ligates to a copper molecule in the active site and the O5 of TPQ points away from the substrate entry channel and the catalytic base (Asp 386 in VAP-1). In the active conformation, the TPQ is flipped 180° from the inactive conformation, the O2 forms a hydrogen bond to a water molecule that interacts with the copper, and the O5 is facing the substrate channel and the catalytic base.
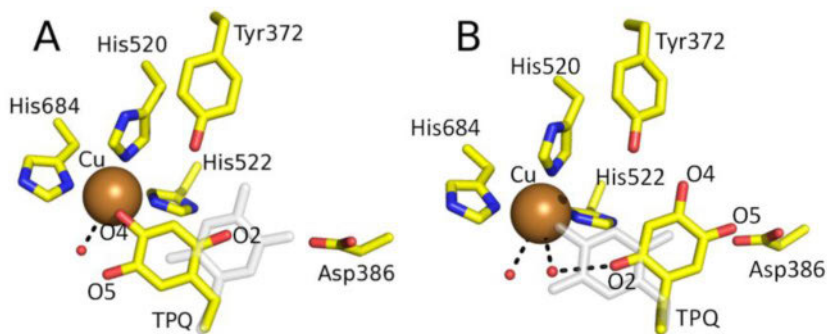
Figure 1. Representation of the two possible TPQ conformations in CAOs. A) On-copper inactive conformation. B) Off-copper active conformation. The transparent TPQ is representing the alternative conformation in both pictures.

The reaction mechanism of CAOs (Figure 2) can be divided into two half-reactions: the reductive and the oxidative half-reactions. The reductive half-reaction is initiated when a substrate amine reacts with the O5 of the oxidized TPQ to form a covalent intermediate; a substrate Schiff base (Mure et al., 2002). A conserved, catalytic Asp residue abstracts the Cα-hydrogen from the substrate molecule yielding a product Schiff base (Wilmot et al., 1997). The product Schiff base is hydrolyzed and the aldehyde product is released, leaving a reduced amine group on TPQ (Su & Klinman, 1998; Wilmot et al., 1999). To reactivate the enzyme, the TPQ is oxidized by molecular oxygen in the oxidative half-reaction. TPQ returns to the resting form and H_2O_2 and NH^{4+} are released.
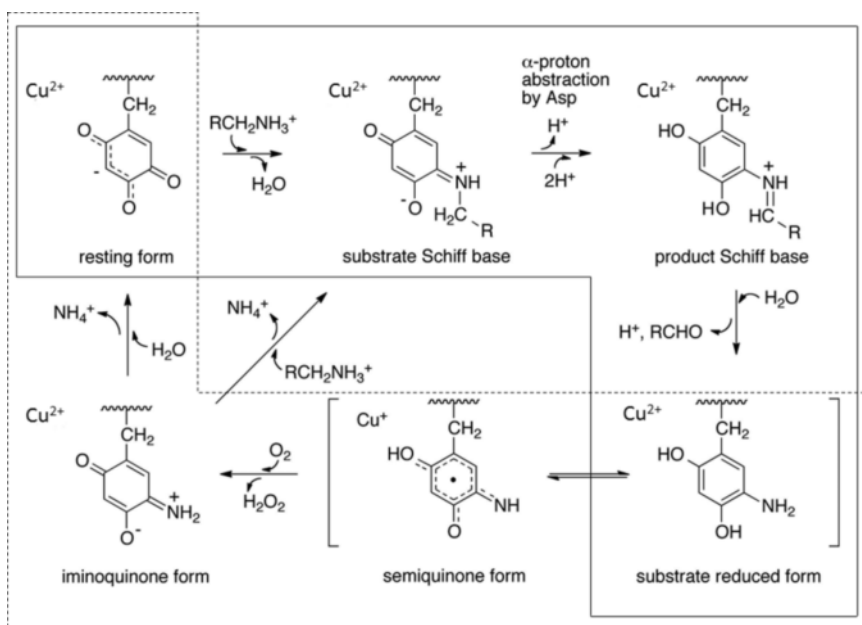
Figure 2. The enzymatic reaction catalyzed by CAOs. The reductive half-reaction is shown in solid box and the oxidative half-reaction is shown in dotted box. (Figure adapted from Mure, 2004 & Finney et al., 2014).

2.4 Structure of VAP-1

The structures of the CAO family members are all homodimers where each monomer is comprised of the three domains; D2, D3 and the catalytically D4 domain (Figure 3A). The crystal structure of human VAP-1 was solved in 2005 by two independent research groups (Airenne et al., 2005; Jakobsson et al., 2005). There were no large differences between the two structures except in the formation of the disulfide bridges, which is probably due to differences in the expression constructs. The structures were solved to 2.5-3.0 Å resolution. All mammalian structures determined to date are listed in Table 1.

The biologically active unit of VAP-1 is a dimer with a heart-shaped structure that is attached to the cell membrane via a transmembrane helix, which is not included in any of the available structures (Figure 3B). The active site of the protein is located deep in the D4 domain, which is the most conserved area. Each subunit of the protein has two long arm-like protrusions, arm I and arm II, which extend from one subunit to embrace the other subunit (Figure 3B). The important residues in the catalytic site are TPQ, the catalytically active base Asp386, and the three His520, His522 and His684 that coordinate the copper ion

16

(Figure 1). Residues from the different domains form a rather long and narrow active site channel leading to the active site. Residues from D2 (85-88) and D3 (173-184, 206-212, 230-239) form one side of the cavity, while residues from arm I of the other subunit (444-450), together with residues from D4 (389, 393-397, 415-426, 467-469, 458-761, 762-673), form the other one.

VAP-1 has an RGD motif (residues 726-728), which is known to function in cell-cell and cell-matrix interactions in integrins (Ruoslahti & Pierschbacher, 1987). In VAP-1 the RGD motif is located on a solvent-exposed tip of a finger-like structure, which is ideal for interactions with a ligand (Airenne et al., 2005). Mutational studies have shown that deletion of the RGD motif diminish but do not abolish the leukocyte adhesion to VAP-1, while only slight variation of the motif (RDG -> RGA) does not cause any differences in leukocyte binding to VAP-1 transfectants (Salmi et al., 2000). The VAP-1 is a glycoprotein and it has been predicted to have six N-linked and three O-linked glycosylation sites (Figure 3B). All six of the N-linked glycosylation sites have been confirmed by X-ray structures and the three glycans on top of the protein are important for the cell adhesion (Airenne et al., 2005; Maula et al., 2005). Two of the glycosylation sites are located near the RDG-motif and the entrance to the active site channel. They might, therefore, control both the enzymatic activity and cell adhesion. The structure is stabilized by a number of intra- and interdomain disulfide bridges.
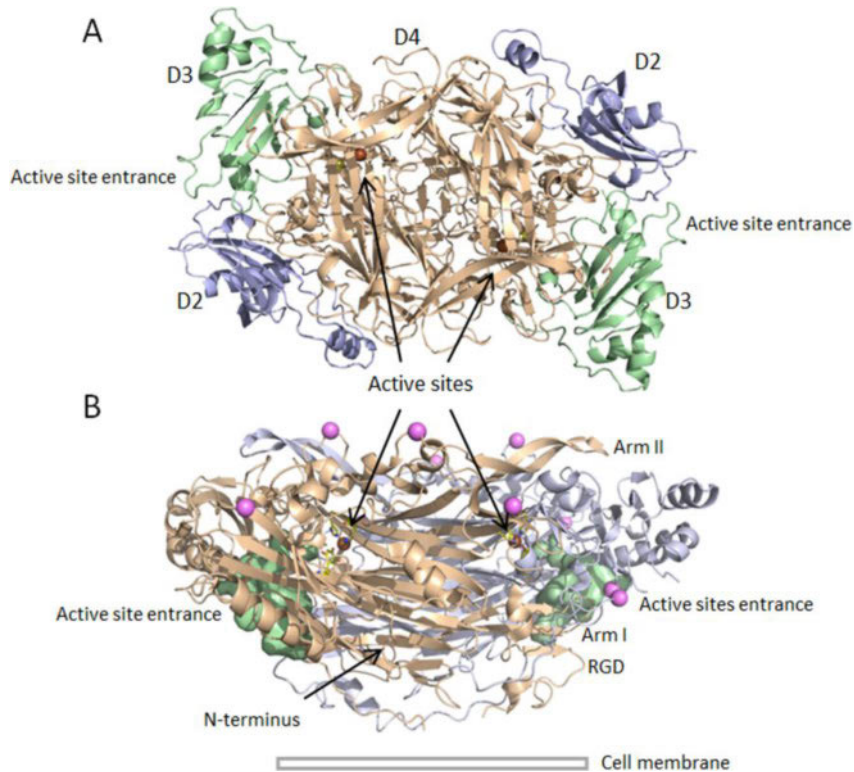
Figure 3. Overall structure of the CAOs. A) Top view of hVAP-1 with the D2 domains shown in blue, the D3 domains shown in green and the D4 domains shown in wheat. B) Side view of the hVAP-1 homodimer, monomers shown in wheat and blue. N-glycosylation sites are shown as purple spheres and the active site cavity is shown in green. VAP-1 has an N-terminal transmembrane helix, which is not visible in the structure. (PDB code 1US1) (Airenne et al., 2005).

2.5 Adhesive function of VAP-1

In addition to the amine oxidase activity, VAP-1 has an adhesive function, as the protein participates in the adhesion of leukocytes to endothelium (Salmi & Jalkanen, 1992; Salmi et al., 1998). Salmi and coworkers discussed about a possible lymphocyte counter-receptor for VAP-1 already in 1992 (Salmi & Jalkanen, 1992). Subsequently, some peptides displaying a suitable free amine group were shown to bind VAP-1 (Yegutkin et al., 2004). Furthermore, Siglec-9 and Siglec-10 have been identified as leukocyte counter-receptors for VAP-1 through phage display screening (Aalto et al., 2011; Kivi et al., 2009). It has been suggested that a free amine group of an arginine in the $C2_2$-domain of the Siglecs can interact with the TPQ of VAP-1. Docking studies with peptides derived from

the predicted interaction region, containing Arg284 and Arg290 in Siglec-9 and Arg293 in Siglec-10, have shown that the peptides can fit in the VAP-1 active site cavity (Aalto et al., 2011; Kivi et al., 2009). However, the finding of Siglec-9 and Siglec-10 as counter receptors for VAP-1 does not exclude the possibility of other binding partners for VAP-1.

Table 1. Available mammalian CAOs structures. The structures from this study are marked with *.

Structure	PDB	Resolution (Å)	Ligand	Reference
DAO	3HI7	1.80		(McGrath et al., 2009)
DAO	3HII	2.15	Pent-amidine	(McGrath et al., 2009)
DAO	3HIG	2.09	Berenil	(McGrath et al., 2009)
DAO	3K5T	2.11		(McGrath et al., 2010a)
DAO	3MPH	2.05	Amino-guanidine	(McGrath et al., 2010b)
VAP-1	1PU4	3.20		(Airenne et al., 2005)
VAP-1	1US1	2.90		(Airenne et al., 2005)
VAP-1	2C10	2.50		(Jakobsson et al., 2005)
VAP-1	2C11	2.90	2HP	(Jakobsson et al., 2005)
VAP-1	2Y73	2.60	Imidazole, on-copper	(Elovaara et al., 2011)*
VAP-1	2Y74	2.95	Imidazole, off-copper	(Elovaara et al., 2011)*
VAP-1	3ALA	2.90		(Ernberg et al., 2010)
VAP-1	4BTW	2.80	Inhibitor **6**	(Bligt-Linden et al., 2013)*
VAP-1	4BTX	2.78	Inhibitor **7**	(Bligt-Linden et al., 2013)*
VAP-1	4BTY	3.10	Inhibitor **13**	(Bligt-Linden et al., 2013)*
bSAO	1TU5	2.37		(Lunelli et al., 2005)
bSAO	2PNC	2.40	Clonidine	(Holt et al., 2008)

2.6 Extravasation of leukocytes to inflamed tissue

For the immune defense to function properly, leukocyte trafficking between the blood, the lymphoid organs and affected tissues is essential. VAP-1 is one of many proteins controlling and participating in the multistep extravasation cascade when leukocytes transmigrate from the blood into tissues (Salmi & Jalkanen, 1992; Salmi & Jalkanen, 2014). *In vitro* binding assays and intraviral microscopy studies have shown that VAP-1 is involved in the rolling, firm adhesion and the transmigration step of the cascade (Figure 4) (Koskinen et al., 2004; Lalor et al., 2002; Salmi et al., 2001; Salmi & Jalkanen, 2001; Stolen et al., 2005; Tohka et al, 2001). According to the current hypothesis, the leukocyte first interacts with VAP-1 through epitopes on Siglec-9 and -10 (Aalto et al., 2011; Kivi et al., 2009) and then the leukocyte slows down, tethers and rolls along the vessel wall. When it arrests, a covalent but transient Schiff base is formed between Siglec and VAP-1. If there are appropriate activation signals, the bound leukocyte transmigrates through the vessel wall and continues toward chemotactic signals within the tissue. The adhesive and enzymatic functions of hVAP-1 are connected since adhesion is reduced when the enzymatic activity is inhibited (Koskinen et al., 2004; Salmi & Jalkanen, 2001).
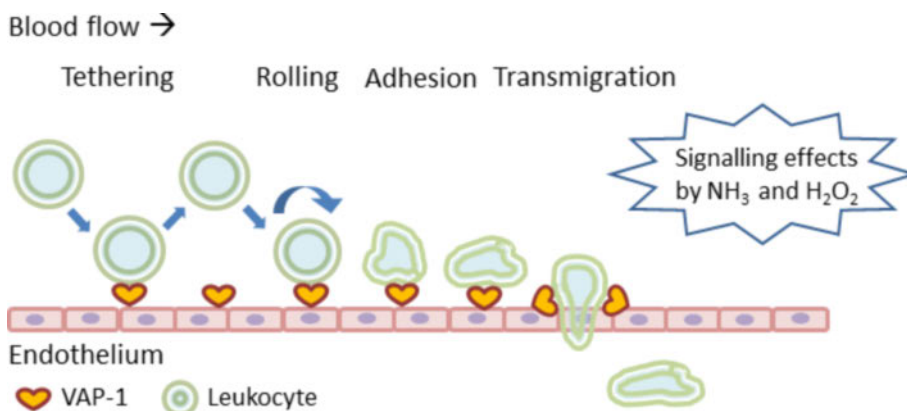
Figure 4. VAP-1 is involved in the rolling, firm adhesion and transmigration step of the extravasation cascade of leukocytes to sites of inflammation.

2.7 VAP-1 in inflammatory diseases

In addition to the direct manner of bringing the leukocyte and endothelial cell in contact with each other during the extravasation of leukocytes to sites of inflammation, VAP-1 can also affect the immune defense in an indirect manner

by altering the environment in a proinflammatory direction via signaling effects. Both the product aldehyde and the side products, hydrogen peroxide and ammonium can induce expression of other endothelial adhesion molecules and chemotactic substances, as well as activation of transcription factors, which further accelerate the inflammation (Jalkanen et al., 2007; Lalor et al., 2007; Liaskou et al., 2011; Salmi et al., 2001). Therefore, VAP-1 activity increases the leukocyte recruitment to the vascular wall, and induces vascular dysfunction by causing direct oxidative damage and also by increasing amyloid aggregation and blood pressure (Jalkanen & Salmi, 2008). The oxidation of lipids through VAP-1–generated hydrogen peroxide can also contribute to vascular damage (Chen et al., 2006; Gokturk et al., 2003).

Inflammation is involved in a wide variety of diseases in the cardiovascular, respiratory, gastrointestinal, musculoskeletal and nervous system (Roivainen et al., 2012) and VAP-1 has been connected to several pathological conditions and diseases. sVAP-1 levels are increased in both insulin-dependent (type 1) and non-insulin-dependent (type 2) diabetes (Garpenstrand et al., 1999; Li et al., 2009a; Salmi et al., 2002). Elevated levels of sVAP-1 have been seen in atherosclerosis (Li et al., 2009b) and VAP-1 activity is connected to preclinical atherosclerosis, affecting the intima-media thickness and carotid plaques (Aalto et al., 2012).

VAP-1 has also been connected to chronic kidney disease (Lin et al., 2008), inflammatory liver diseases (Kurkijarvi et al., 1998; Lalor et al., 2007) and congestive heart failure (Boomsma et al., 1997). It has been shown that VAP-1 is important in the pathogenesis of arthritis (Marttila-Ichihara et al., 2006) and elevated VAP-1 levels have been detected in patients with systemic sclerosis (Yanaba et al., 2013), multiple sclerosis (Airas et al., 2006) and psoriasis (Madej et al., 2007). VAP-1 appears to play an important role in the development of liver fibrosis (Weston et al., 2015) and in allergic inflammatory responses of the airways (Dunkel et al., 2014). It has been connected to acute ocular inflammation, ocular angiogenesis and pathophysiology (Noda et al., 2008a; Noda et al., 2008b). Moreover, VAP-1 is involved in nonclassical inflammatory diseases like cancer. VAP-1 gene amplification has been detected in the genome of gastric cancer patients (Varis et al., 2002) and VAP-1 activity is upregulated in colorectal cancer tissues (Li et al., 2014). Specimens from head, neck, liver and melanoma tumors also show increased VAP-1 expression (Forster-Horvath et al., 2004; Irjala et al, 2001; Yoong et al., 1998).

In vitro and *in vivo* studies have clarified several aspects of the VAP-1 function. In VAP-1 deficient mice (knock out) the cell migration during inflammation is decreased (Stolen et al., 2005) and tumors grow more slowly (Marttila-Ichihara et al., 2009). Overexpression of VAP-1 at the cell surface of endothelial cells leads to increased binding of lymphocytes affecting the transmigration cascade. Studies have also shown that the oxidase activity of the protein is of importance in neoangiogenesis, cell recruitment, tumor growth and inflammation (Marttila-Ichihara et al., 2009; Noonan et al., 2013). The VAP-1 activity is dependent on the oxidase activity and, moreover, the oxidase activity is entirely dependent on the TPQ, as mutagenesis of this residue abolishes all catalytic activity of VAP-1 (Koskinen et al., 2007; Noonan et al., 2013). To summarize, these data show that the enzymatic activity of VAP-1 is crucial in leukocyte migration (Salmi & Jalkanen, 2014).

2.8 VAP-1 as drug target

As inflammation is involved in a wide variety of diseases involving for example the cardiovascular, respiratory, gastrointestinal, and nervous system, there is a great need for anti-inflammatory therapy. VAP-1 and its involvement in the leukocyte trafficking to sites of inflammation make it an attractive drug target (Smith & Vainio, 2007). The impact of VAP-1 immunotherapy is much needed as chronic inflammatory diseases increase in Western industrialized countries due to the socioeconomically standard and aging population (Thorburn et al., 2014; MacNee et al., 2014).

The dual function of VAP-1 gives it advantages as drug target over other adhesion receptors, since both the adhesive and enzymatic activity can be inhibited (Salmi & Jalkanen, 2005). The catalytic center of an enzyme presents a good starting point for rational drug design as analogues of known substrates and inhibitors can be designed and developed. Available crystal structures further aids in the planning of novel inhibitors. The fact that the adhesive function of VAP-1 is inhibited by small molecular inhibitors, which can be administered orally, is a clear benefit over drugs that need to be injected intravenously or subcutaneously (Jalkanen & Salmi, 2008).

In order to block the function of VAP-1, it is critical to understand the function of the protein at the molecular level (Finney et al., 2014). Both small molecular

inhibitors and antibodies have proven successful and effective in inhibiting leukocyte-endothelial cell interactions in several disease models (Koskinen et al., 2004; Lalor et al., 2002). Alleviation of disease state and leukocyte trafficking has been seen in the following models: liver transplantation (Martelius et al., 2004; Martelius et al., 2008), liver fibrosis (Weston et al., 2015), arthritis (Marttila-Ichihara et al., 2006), lung inflammation (Foot et al., 2012; Foot et al., 2013; O'Rourke et al., 2008) and in encephalomyelitis in mice which shares characteristics with human multiple sclerosis (O'Rourke et al., 2007).

Recently, VAP-1 has also emerged as a target for *in vivo* imaging of inflammation (Aalto et al., 2011; Li et al., 2013; Luo et al., 2013; Roivainen et al., 2012). Utilizing the detection of inflammation-induced luminal VAP-1 as an imaging target could have major clinical impact, and the method can be used as a diagnostic tool for the detection and characterization of inflammatory diseases. Positron emission tomography (PET) imaging with a ^{68}Ga-labelled peptide of Siglec-9 has been shown to detect VAP-1 in vasculature at sites of inflammation and cancer (Aalto et al., 2011).

2.9.1 Anti-VAP-1 antibodies

It has been shown both *in vitro* and *in vivo* that anti-VAP-1 antibodies can block the adhesive function of VAP-1 to promote leukocyte transmigration in humans and, thus, reduce the migration of leukocytes. It has also been shown that the antibody-mediated inhibition did not lead to any side effects in the immune system (Kirton et al., 2005, Koskinen et al., 2007). Monoclonal antibodies bind to VAP-1 in an area, which does not inhibit the oxidase activity of the protein (Koskinen et al., 2004; Bonder et al., 2005; Merinen et al., 2005). Function-blocking antibodies reduce the number of infiltrating leukocytes in acute and chronic inflammatory models including dermatitis (Vainio et al., 2005), peritonitis (Merinen et al., 2005), liver rejection, and hepatitis (Bonder et al., 2005; Martelius et al., 2004). Humanized and function-blocking anti-VAP-1 antibodies have also been produced (Autio et al., 2013; Kirton et al., 2005). BTT-1023 has shown efficacy and safety in clinical studies in arthritis and psoriasis patients (Autio et al., 2013). It has also shown efficacy in a range of preclinical models of inflammatory diseases, including chronic obstructive pulmonary disease, certain neurological conditions, and certain niche liver inflammatory fibrotic diseases. Currently, BTT-1023 is undergoing phase 2 clinical trials (Autio et al., 2013).

2.9.2 Small molecular inhibitors

CAO activity can be inhibited by carbonyl reactive groups such as semicarbazide (Figure 6A) and hydrazines (Lyles, 1996). The hydrazines were initially designed to inhibit MAO A and MAO B, but they also inhibit CAOs, such as VAP-1 and DAO (Lizcano et al., 1996). Therefore, they are not specific and they bind irreversibly, which is not a desirable feature. Thereafter, different types of small molecules have been developed that can be grouped into two main classes: irreversible mechanism based inhibitors (Figure 5A, B, C D&E) and noncovalent/reversibly binding inhibitors (Figure 5F&G) (McDonald et al., 2007; Dunkel et al., 2011). The irreversible inhibitors are either based on allylamines (Figure 5B&C) or hydrazines (Figure 5D&E). Other molecules known to inhibit VAP-1 are: amino acid derivatives, benzamides, oxime-based SSAO inhibitors, aminoglycoside antibiotics, vitamin B1 derivatives, and peptides (Dunkel et al., 2008; Dunkel et al., 2011). More recently developed inhibitors, such as, ELP 12, LJP1207, PXS-4861A, BTT-2052 and LJP1586 have proven specificity and potency for VAP-1 (Figure 5) (Bonaiuto et al., 2012; Wang et al., 2006; Foot et al., 2013; Marttila-Ichihara et al., 2006; O'Rourke et al., 2008).
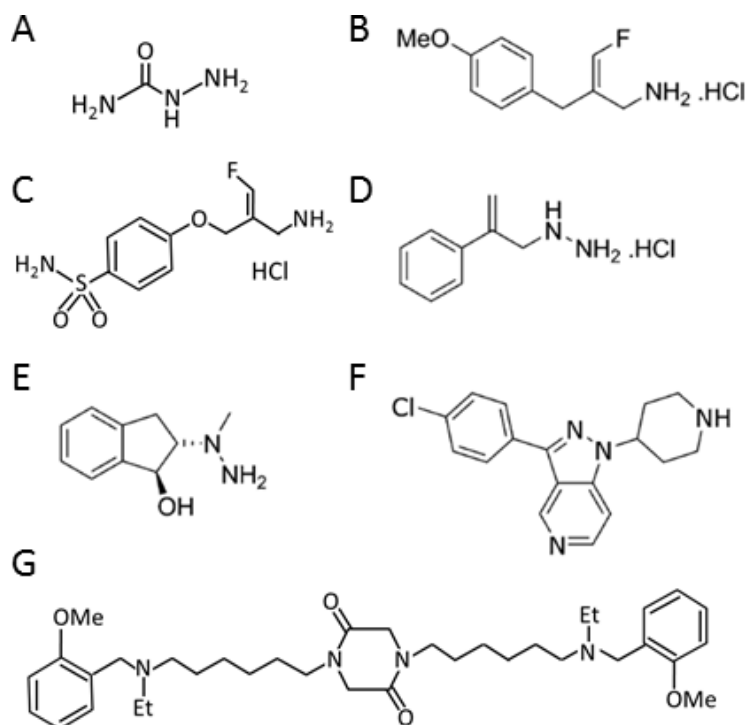
Figure 5. Examples of VAP-1 inhibitors. A) Semicarbazide. B) LJP1586. C) PXS-4681A. D) LJP1207. E) BTT-2025. F) 3-phenyl-1-*H*-pyrazoleo[4,3-c]-pyridine. G) ELP 12.

2.9.3 CAO structures in complex with inhibitors

The crystal structure of human VAP-1 in complex with the irreversible inhibitor 2-hydrazinopyridine (2HP; PDB code 2C11) shows a covalent bond between the C5 atom of TPQ and the inhibitor, which forms a substrate Schiff base mimic (Figure S5E of Supporting Information in publication I) (Jakobsson et al., 2005). As 2HP contains nitrogen instead of a carbon at the C1 position, the covalent complex formed with the inhibitor cannot be deprotonated and, thus, accumulates in the crystal. Therefore, the hydrazine compounds are suicide inhibitors and once they react with TPQ, they cannot be released from the catalytic site.

bSAO and DAO have both been crystallized with non-covalently bound inhibitors. Holt and coworkers solved the complex structure of bSAO and clonidine (Figure S5C of Supporting Information in publication I) (PDB code 2PNC) (Holt et al., 2008). The inhibitor-bound structure does not show any major differences compared to the native structure, except that Asn469 has

rotated 180° in the active site channel to allow binding of clonidine. The aromatic ring of clonidine π-stacks with TPQ and Tyr 472, while two nitrogen atoms of clonidine hydrogen bond to Tyr383 and the catalytic base Asp385. The catalytic base, Asp386 in DAO is also hydrogen bonding the non-covalently bound inhibitors berenil and pentamidine in the complex structures of DAO (Figure 3 in publication II) (PDB codes 3HIG and 3HII) (McGrath et al., 2009). Asp186 in the active site channel is involved in interaction with pentamidine and both inhibitors π-stack with Trp376 and Tyr371. Berenil binds in an extended conformation, while pentamidine adopts a bent horseshoe conformation. Based on the analysis of previous CAO inhibitors, and the binding mode of irreversible VAP-1 inhibitors, it would be advantageous to develop reversible VAP-1 inhibitors.

3. AIMS OF THE STUDY

The overall goal of this study was to understand the structural and functional properties of the active site in CAOs, especially in VAP-1. As VAP-1 is a known drug target in inflammatory diseases, the primary aim was to study the VAP-1-ligand interaction at atomic level. New insight in the ligand interactions of CAOs and VAP-1 is valuable in the drug development against these targets.

The specific aims were as follows:

I. To analyze the structural properties of VAP-1 with X-ray crystallography and to study the active sites of VAP-1 and RAO to understand their differences in substrate preference (Publication I).

II. To evaluate the molecular interaction between VAP-1 and potent inhibitors targeted to the novel binding site of VAP-1 discovered in Publication I (Publication II).

III. To identify the underlying reasons for species specific binding of ligands in VAP-1 (Publication III).

IV. To study the evolutionary relationship of mammalian CAO in detail, to identify and classify new and poorly characterized CAOs and derive general rules for substrate specificity in this class of enzymes (Publication IV).

4. MATERIAL AND METHODS

The material and methods that were used in this study are described in full detail in the respective publication (I-IV). The brief descriptions below are presented to give an overview.

4.1 Crystallography

4.1.1 Extraction of VAP-1 for crystallization (I, II)

The soluble form of VAP-1 was extracted and purified from human serum by Biotie Therapies Corp. The sample was dialyzed against 10 mM potassium phosphate (pH 7.2) and prior to crystallization the protein was concentrated in Eppendorf concentrators by centrifugation at 12000 rpm at 4° to approximately 1.0 mg/ml. The protein was stored at 4°.

4.1.2 Crystallization and diffraction data collection (I, II)

The protein was crystallized using the hanging drop vapor diffusion technique at room temperature. The imidazole complexes were crystallized by mixing the protein with a well solution of 0.7 M Na/K tartrate, 100 mM imidazole (pH 7.4), and 200 mM NaCl (Publication I). For co-crystallization of the inhibitor complexes VAP-1 was incubated with the inhibitors for 1 h at 37° in a 1:10 molar ratio prior to crystallization setup. The crystals grew in a crystallization condition containing protein and 0.7 Na/K tartrate, 0.2 M NaCl, 0.1 M Hepes, pH 7.4-7.6, and 200 mM NaCl (Publication II). Before data collection the crystals were dipped in a cryoprotectant of 0.6−0.8 M Na/K tartrate, 0.2 M NaCl, 0.1 M Hepes, pH 7.6, 1.3−2 M Na formate and 100 mM imidazole (Publication I) or 0.05 mM of inhibitor (Publication II), and then cryocooled in liquid nitrogen. Diffraction data collection was carried out at MAX-lab (Lund, Sweden) (Publication I) and European Synchrotron Radiation Facility (Grenoble, France) (Publication II).

4.1.3 Data processing, structure solution and refinement (I, II)

XDS (Publication I) (Kabsch, 2010) and HKL3000 (Publication II) (Otwinowski & Minor, 1997) were used for processing of the diffraction data. All structures belonged to the $P6_{5}22$ space group. The structures were solved with molecular

replacement using the CCP4i program suite (Dodson et al., 1997) with the dimer of human VAP-1 structure (PDB code 1US1) (Airenne et al., 2005) as the search model. Inhibitor crystals showed significant anisotropy. During data processing, due to very weak diffraction and a low signal-to-noise ratio, the threshold for peak search was changed in order for the autoindexing to work for the VAP-1-**13**-complex in publication II. Computational corrections for absorption in a crystal, corrections for minor misalignment of the goniostat, together with corrections for anisotropic diffraction, were all implied during data processing of the VAP-1-inhibitor structures (Publication II) (Borek et al., 2003; Borek et al., 2010; Borek et al., 2013; Dodson et al., 1997). Refinement was done with REFMAC5 (Publication I & II) (Murshudov et al., 1997) and PHENIX (Publication I) (Adams et al., 2010). The structures were rebuilt in COOT (Emsley & Cowtan, 2004) and assessed with Molprobity (Davis et al., 2007). Pymol (DeLano, 2008) was used to analyze and visualize the structures and to make figures.

4.2 Activity measurements of VAP-1 activity

The activity measurements were done by collaborators in Sirpa Jalkanen's research group or BioTie Therapies Corp. The inhibitors in publication II were designed and synthesized by BioTie Therapies Corp. and Ferenc Fülöp's research group.

4.2.1 Protein expression for activity measurements (I, II)

The recombinant VAP-1 used in the VAP-1 activity and inhibition measurements was expressed in either Chinese hamster ovary cell lines for hVAP-1 (CHO-VAP-1), which have previously been reported (Smith et al., 1998), or Hamster embryonic kidney (HEK) 293 EBNA cells (Publication I & II). The CHO cells are stably transfected with a full-length human VAP-1 cDNA. The corresponding recombinant mouse VAP-1 and cynomolgus monkey VAP-1 proteins were also obtained from CHO cells (Publication II). Rat MAO was prepared from rat liver (Nurminen et al., 2011) and purified human MAO A and MAO B were purchased from Sigma-Aldrich (Publication II).

4.2.2 Inhibition with imidazole and inhibitors (I, II)

The role of imidazole on VAP-1 activity was determined radiochemically with CHO-VAP-1 lysate and labeled benzylamine based on the method of Fowler and

Tipton (Publication I) (Fowler and Tipton, 1981). The *in vitro* inhibition of VAP-1 activity with inhibitors was tested with a coupled colorimetric method where the measured increase in absorbance during the experiment reflects the VAP-1 activity (Publication II) (Holt et al., 1997; Nurminen et al., 2010; Nurminen et al., 2011). MAO activity and inhibition thereof was tested in the same way, with exception of the substrate (tyramine for MAO and benzylamine for VAP-1). The binding kinetics of inhibitors **6** and **7** to VAP-1 were analyzed in a binding assay with a Biacore T100 instrument where recombinant purified VAP-1 was amine coupled to a CM5 sensor chip (Publication II).

4.2.3 Enzyme activity assays for VAP-1 mutants (I)

The activity of VAP-1 mutants was determined by correlating it to the changes in their H_2O_2 production with and without semicarbazide inhibition (Publication I). The H_2O_2 production was quantified using an Amplex Red-labeled phenoxazine reagent and fluoropolarometer (Salmi et al., 2001).

4.3 Modeling (II, III, IV)

All sequences were retrieved from the UniProt Knowledgebase (The UniProt Consortium, 2015): mouse VAP-1 (O70423), rat VAP-1 (O08590), monkey VAP-1 (G7PUW6) and human RAO (O75106). hVAP-1 (PDB code 2Y74) and hVAP-1 in complex with inhibitor **13** (PDB code 4BTW) were used as template structures in publications II and III. hVAP-1 (PDB code 4BTX) was used as template to model RAO in publication IV. BODIL and MALIGN were used for sequence alignment (Lehtonen et al., 2004) and MODELLER (Sali & Blundell, 1993) was used to generate the homology models. For each protein, ten models were generated, and in each case, the model with the lowest energy based on the objective function was chosen for further analysis. Surfnet (Laskowski, 1995) and Mask were used to calculate the active site cavities and to extract the residues lining the binding site.

4.4 Phylogenetic studies (IV)

The phylogenetic study was done by my co-author, PhD student Leonor Lopes de Carvalho. Sequences for DAO (UniProtKB code: P19801), RAO (O75106), VAP-1 (Q16853) and bSAO (Q9TTK6) proteins, were obtained from the UniProt knowledgebase (Uniprot consortium 2015). To identify potential CAOs several BLAST searches (Altschul et al., 1990) were done using hDAO, hRAO,

hVAP-1 and bSAO as query against mammalian genomes with the protein blast program provided by the National Center for Biotechnology Information (NCBI, http://blast.ncbi.nlm.nih.gov). The phylogenetic reconstruction was performed using MEGA5 (Tamura et al., 2011) and calculated with Neighbor-Joining (NJ) (Saitou & Nei, 1987) and Maximum Likelihood methods (ML). The Jones-Taylor-Thornton (JTT) (Jones et al., 1992) substitution matrix was used to generate the trees. The topologies of the trees were inferred with bootstrap consensus trees using 500 replications (Felsenstein, 1985). Multivariate analysis (PCA, MS Johnson) was also done based on the phylogenetic distance data in MEGA5.

5. RESULTS

5.1 Serum VAP-1 in complex with imidazole (I)

5.1.1 Serum VAP-1 crystal structure (I)

We determined the first three dimensional structure of cleaved soluble serum VAP-1 with X-ray crystallography. Two crystal structures of hVAP-1 were refined to 2.60 and 2.95 Å with final Rfactors of 17.5% (Rfree = 21.3%) and 17.9% (Rfree = 21.4%) (Table 1 in I). Two imidazole molecules originating from the crystallization buffer were bound in both hVAP-1 structures, one molecule (Imid1) at TPQ and another (Imid2) in the active site channel. Overall, the structures are similar with a root-mean-square deviation (rmsd) of 0.12 Å for 1200 Cα atoms, but TPQ in the active site is interacting with Imid1 in different ways (Figure 6). In the 2.60 Å structure the TPQ in inactive on-copper conformation hydrogen bonds to Imid1 (Figure 6A), while in the 2.95 Å structure the TPQ in active off-copper conformation is covalently bound to Imid1 (Figure 6B). Asp386 also forms a hydrogen bond with Imid1 in both structures.
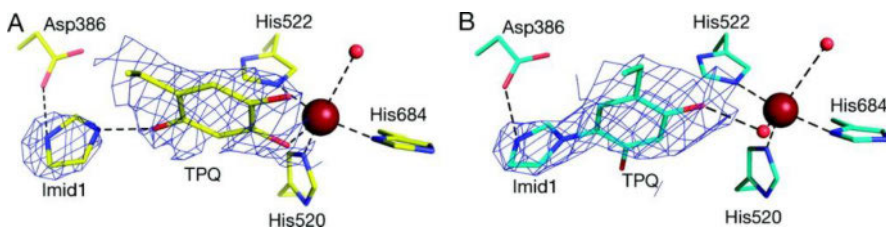
Figure 6. TPQ conformations of the sVAP-1 structures. A) In the on-copper inactive conformation, imidazole (Imid1) is hydrogen bonded to TPQ (PDB code 2Y73). B) In the off-copper active conformation, imidazole (Imid1) is covalently bonded to TPQ (PDB code 2Y74). The omit maps for TPQ and Imid1 are contoured at σ level 1.0. (Publication I, Figure 1)

5.1.2 Identification of a secondary imidazole binding site (I)

A novel secondary imidazole binding site was determined as an imidazole molecule (Imid2) could be modeled in the active site channel (Figure 7). The Imid2 forms a hydrogen bond to Tyr394 and a water-mediated contact with the main chain nitrogen of Thr212 in all chains of both structures. The OH group of Thr212 in chain B of the on-copper structure is also making a water-mediated

hydrogen bond to Imid2 (Figure 7A), while the Thr212 side chain has flipped and participates in a hydrogen bonding network with Arg216 and Tyr176 in both chains of the off-copper structure and in chain A of the on-copper structure (Figure 7B). Additionally, Leu469 and Tyr176 form hydrophobic contacts with Imid2.
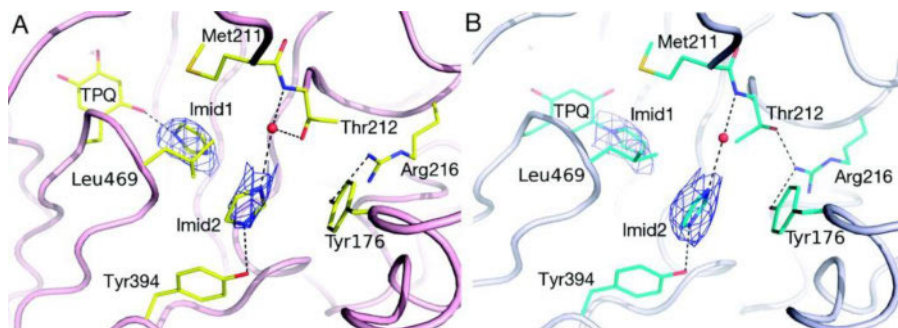
Figure 7. The novel secondary imidazole binding site in the active site channel of hVAP-1. A) Thr212 side chain makes a water-mediated interaction to the imidazole (Imid 2) bound in the active site channel (PDB code 2Y73). B) Thr212 side chain is hydrogen bonded to Arg216 in the off-copper structure (PDB code 2Y74). Tyr394 is hydrogen bonded to Imid2 in both structures. The omit maps for Imid1 and Imid2 are contoured at σ level 1.0. (Publication I, Figure 2)

5.1.3 Imidazole inhibits VAP-1 enzymatic activity (I)

The effect of imidazole on VAP-1 activity was tested in an assay by monitoring the formation of radioactive benzylaldehyde from 14C-labeled benzylamine. Imidazole clearly inhibits the hVAP-1 enzymatic activity with an IC_{50} of 1.28-8.6 mM (95% confidence interval) (Figure 4 in I). A 100 mM imidazole concentration, which corresponds to the crystallization setup, inhibits 93% of the hVAP-1 activity.

5.2 Pyridazinone inhibitors of VAP-1 (II)

5.2.1 Potent pyridazinone inhibitors of VAP-1 (II)

To target the secondary imidazole binding site in the active site channel, a novel set of pyridazinone inhibitors was designed and synthesized (Figure 8) (Scheme 1 and 2 in II). *In vitro* activity testing of inhibitors **6**, **7** and **13** with recombinant VAP-1 show that the compounds are very potent against human VAP-1 enzyme activity, having IC_{50} values from 290 to 20 nM (Table 1 in I). Inhibitor **13** is the

most potent human VAP-1 inhibitor with an IC_{50} value of 20 nM, while inhibitor **6** has an IC_{50} value of 71 nM and inhibitor **7** has the lowest activity with an IC_{50} value of 290 nM. The biacore surface plasmon resonance analysis demonstrates a high affinity binding ($K_D = 0.17 \times 10^{-6}$ M for **6** and $K_D = 0.20 \times 10^{-6}$ M for **7**) with very fast association kinetics ($k_a = 1.00 \times 10^{-6}$ M^{-1} s^{-1} for 6 and $k_a = 1.88 \times 10^{-6}$ M^{-1} s^{-1} for **7**) and moderate dissociation kinetics ($k_d = 0.17 \times 10^{-6}$ s^{-1} for **6** and $k_d = 0.38 \times 10^{-6}$ for **7**) when hVAP-1 is immobilized on a chip. The kinetic studies confirm that the inhibitors bind reversible to VAP-1.
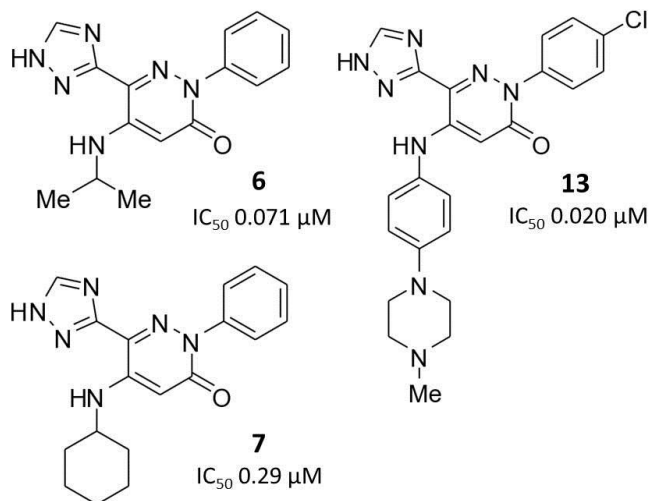
Figure 8. The structures of the pyridazinone inhibitors **6**, **7** and **13**.

5.2.2 The inhibitors present a novel binding mode to VAP-1 (II)

To study the binding mode of inhibitors **6**, **7** and **13** at a molecular level, they were co-crystallized with hVAP-1 and their crystal structures were determined. The structures were refined to 2.80 Å, 2.78 Å, and 3.10 Å resolution, with R-factors of 20.5% (*Rfree* of 26.0%), 17.4% (*Rfree* of 23.6%), and 18.5% (*Rfree* of 25.0%), respectively (Table 2 in publication II). All crystals showed significant anisotropy, and correction for this was especially important for successful data processing and quality of the final electron density maps. Despite the anisotropy, the electron density was good throughout the structures (Supporting Information Figure 2A&B in II).

The X-ray structures reveal that inhibitors **6**, **7**, and **13** bind in the active site channel (Figure 9A-E), close to the previously determined secondary imidazole

binding site (Figure 9F). The TPQ is in active off-copper conformation in all the chains of the complex structures and the structures are similar with an rmsd of 0.28-0.40 Å after superimposition. All three inhibitors bind noncovalently to hVAP-1 through hydrogen bonds, π-stacking, and hydrophobic interactions. Due to similar scaffold, the inhibitors show a similar reversible binding mode with only minor differences (Figure 9). Tyr394, Asp180, and Thr212 form hydrogen bonds to all the inhibitors. Tyr176 π-stacks to the pyridazinone of all inhibitors and Phe389 makes a T-shaped π-stacking with the phenyl ring of inhibitors **6** and **7**, as well as a Cl−π interaction with inhibitor **13**. Tyr448 on arm I originating from the other monomer make a hydrogen bond with all inhibitors and Phe173, Leu177, Leu468, and Leu469 interact hydrophobically with the inhibitors. The side chain of Thr212 in all B chains make hydrogen bonds through a water molecule to the inhibitors (Figure 9D), while in all A chains the side chain is flipped 180° and does not interact with the inhibitors (Figure 9B,C,E). Similar to the interactions of the Thr212 side chain in the on-copper imidazole structure, Thr212 in all A chains of the VAP-1-inhibitor complex structures forms a hydrogen bond to Arg216. The secondary imidazole binding site and the inhibitor binding site are overlapping (Figure 9F). However, there are differences as the imidazole moiety of the inhibitors is not exactly in the same position as the Imid2 in the sVAP-1 structures. Imid2 and the inhibitors are binding in close proximity of each other in the channel and Tyr394 interact with hydrogen bonds to both Imid2 in the sVAP-1 structures and all three VAP-1 inhibitor structures (Figure 9F).
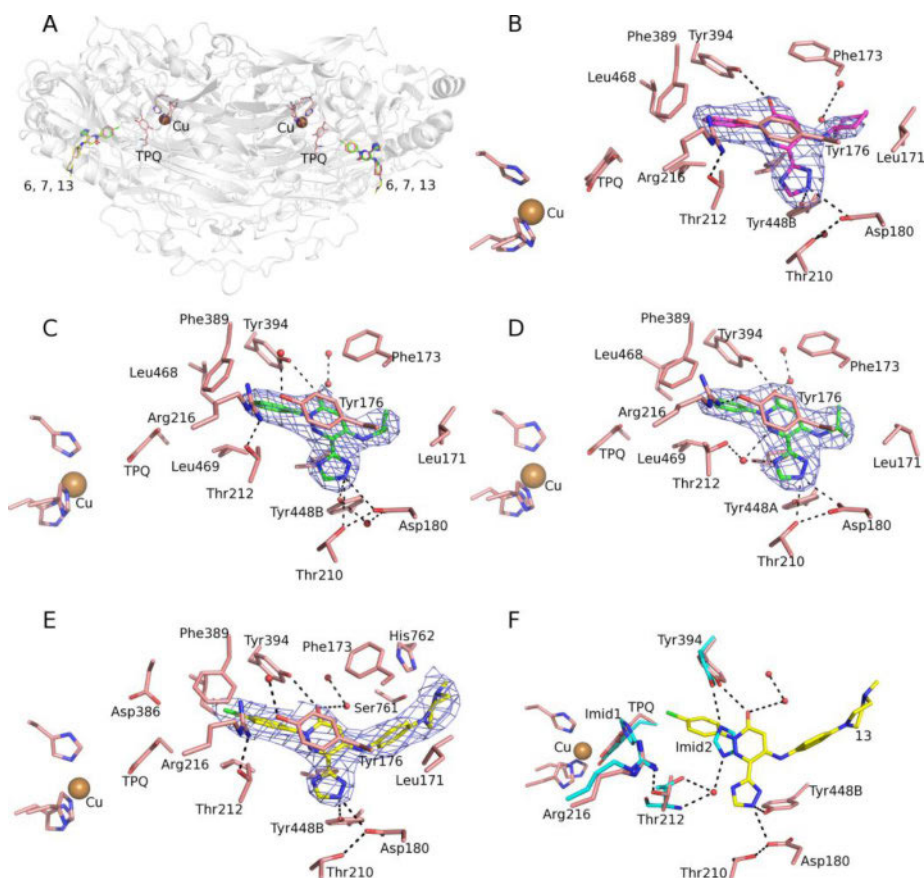
Figure 9. Molecular binding mode for inhibitors **6**, **7**, and **13** in hVAP-1. A) Overall view of the VAP-1 inhibitor complexes. The inhibitors bind in the active site channel and block the access to the TPQ. B) Binding mode for inhibitor **6** (PDB code 4BTY). C) Binding mode for inhibitor **7** (PDB code 4BTX). Thr212 makes hydrogen bond to Arg216. D) Binding mode of **7** in chain B, where Thr212 is involved in a water-mediated hydrogen bond to the inhibitor. E) Binding mode for inhibitor **13** (PDB code 4BTW). F) Comparison of imidazole (Imid2) bound in the secondary imidazole binding site and the binding site for inhibitor **13**. The σ-weighted $2F_o - F_c$ electron density maps are contoured at 1.5 σ in C–E and at 1.0 σ in B. (Adapted from Publication II, Figure 2.)

5.2.3 The inhibitors show specificity for VAP-1 over other CAOs (II)

In addition to the high potency for the human VAP-1, the pyridazinone inhibitors have excellent specificity for VAP-1 over other CAOs like MAO and DAO (Table 1 in II). Only 3-18% of total rat MAO activity was inhibited at 100

μM concentration and inhibition data for inhibitors **6** and **13** show similar results for human MAO A and human MAO B with 20 μM inhibitor concentration. Inhibitor **6** and **7** inhibits 40% and 30% of DAO activity at 100 μM concentration, respectively, while inhibitor **13** inhibits 36% of DAO activity at 50 μM concentration.

5.2.4 The inhibitors are weak inhibitors of mouse VAP-1 activity (II)

Even though inhibitors **6**, **7**, and **13** are potent hVAP-1 inhibitors they are surprisingly weak inhibitors of mouse VAP-1 activity (Figure 10). Inhibitor **6** and inhibitor **13** show a similar effect with 24% and 23% inhibition of the mouse VAP-1 activity, while inhibitor **7** shows the lowest inhibitory effect with a 10% inhibition of the mouse VAP-1 activity. Enzymes of rodent species such as rat, guinea pig and hamster also show lack of VAP-1 inhibition by the pyridazinone inhibitors. However, the potency against the enzyme of another primate, cynomolgus monkey, is very similar to human VAP-1 for all three inhibitors with IC_{50} values of 26-250 nM (Table 1 in II).
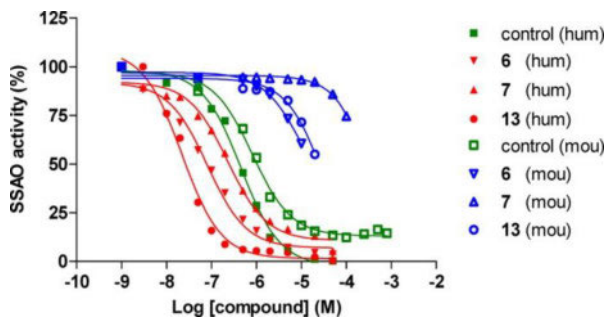
Figure 10. hVAP-1 and mouse VAP-1 activity inhibition by inhibitors **6**, **7** and **13**. The inhibitors are very potent against hVAP-1 but do not inhibit mouse VAP-1 well. (Publication II, Figure 1)

5.3 Structural comparison of rodent and primate VAP-1 active site (II, III)

5.3.1 Differences affecting the architecture of the active site (III)

To identify differences in primate and rodent VAP-1 active site, which could explain the species specific ligand binding seen in publication II, sequence alignments and homology models of the proteins were generated. Homology models of mouse, rat, and cynomolgus monkey VAP-1 were made based on the

hVAP-1 crystal structure. The overall fold of the proteins is very similar due to high sequence identities, 83% for mouse, 82% for rat and 96% for monkey compared to human VAP-1. The sequence identity between the mouse and rat VAP-1 sequence is very high, 93%. Residues lining the active site cavity were derived with the program Mask, and the residues that differ among the 4 species are listed in Table 2. There are no differences in the primary binding site close to TPQ. However, around the secondary imidazole binding site and where the pyridazinone inhibitors bind, there are several substitutions that affect the architecture of the active site channel.

Looking at the shape of the active site cavities, there are clear differences between primate and rodent VAP-1 (Figure 11A&B). The cavity is narrower in the rodents because of the Leu447^{primate}/Phe^{rodent} substitution, as the Phe is larger and occupies more space than the Leu in the primate protein. This residue is actually placed on the tip of Arm I coming from the other monomer of the protein. Three substitutions, Phe173^{primate}/Thr^{rat}/Asp^{mouse}, Leu177^{primate}/Gln^{rodent} and Asp180^{primate}/Gln^{rat}/Glu^{mouse} are located on α-helix5 of the D3 domain at the entrance to the active site channel. Furthermore, Thr210^{primate}/Lys^{rat} substitution in rat VAP-1 affects the shape of the active site. There is, however, only one single difference between the human and monkey VAP-1, Thr212^{human}/Asn^{monkey}.

5.3.2 Key substitutions causing species specific binding (II)

Even though the pyridazinone inhibitors are potent against human VAP-1, they are only weak inhibitors of mouse VAP-1, with a 10-24% inhibition of mouse VAP-1 activity. A homology model of mouse VAP-1 in complex with inhibitor **13** (done based on the hVAP-1-**13**-complex structure) shows the key substitutions in the active site channel (Figure 11C). Inhibitor **13** is bound in the channel exactly where the Arm I from the other monomer reach into the active site. The Leu477B^{human}/Phe^{mouse} substitution will, therefore, affect the inhibitor binding. The Phe173^{human}/Asp^{mouse} substitution together with His762^{human}/Tyr^{mouse} affects inhibitor binding as the 173Asp^{mouse} and 762Tyr^{mouse} form a hydrogen bond and restricting the entrance to the active site. The corresponding residues, 173Phe^{human} and 762His^{human}, cannot create a similar hydrogen bond with each other. Tyr448B^{human} and Asp180^{human} are both hydrogen-bonded to the inhibitor, but in mouse VAP-1 the corresponding residues are not at all interacting with the inhibitor. The Val209^{human}/Leu^{mouse} substitution will cause the conserved Tyr448B$^{human/mouse}$ into a slightly different conformation in the mouse VAP-1,

where it can hydrogen bond to Glu180^{mouse}, which is corresponding to Asp180^{human}.

Table 2. Residues lining the active site channel of VAP-1 from human, monkey, rat, and mouse that differ between the species. The residues causing significant differences in the channel properties are marked with an asterisk. The residues are colored by hydrophobicity (blue=most hydrophobic and red = most hydrophilic). (Publication III, Table I)

Residue number	Human	Monkey	Rat	Mouse
Chain A				
173*	Phe	Phe	Thr	Asp
177*	Leu	Leu	Gln	Gln
180*	Asp	Asp	Gln	Glu
210*	Thr	Thr	Lys	Thr
212	Thr	Asn	Thr	Thr
239	Phe	Phe	Tyr	Tyr
388	Gly	Gly	Ser	Ser
395	Thr	Thr	Ser	Ser
425	Ile	Ile	Leu	Leu
761*	Ser	Ser	Thr	Ala
Chain B				
447*	Leu	Leu	Phe	Phe
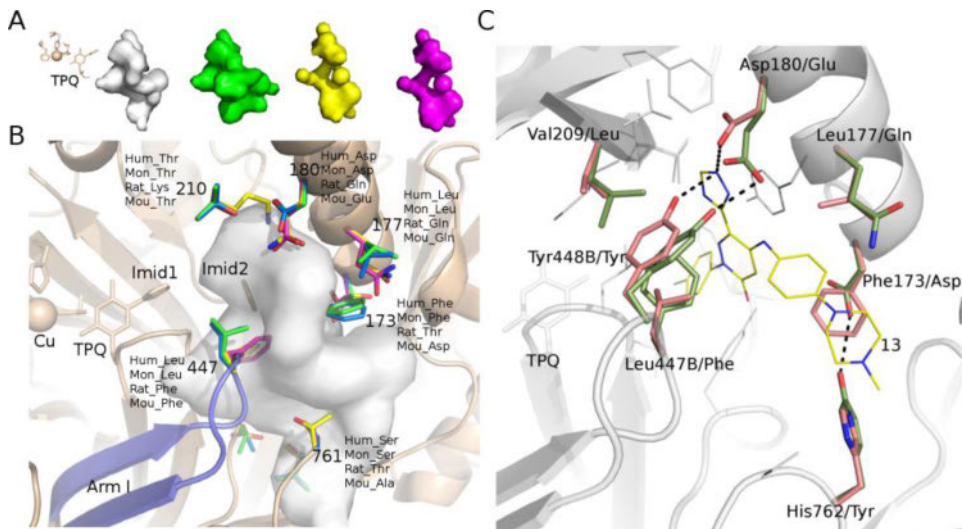
Figure 11. The active site cavity in mammalian VAP-1. A) The shape of the active site cavity in human, monkey, rat, and mouse VAP-1. B) Arm I (blue) from the other subunit of the dimer is lining the active site cavity and the Leu447[human]/Phe[mouse] substitution in the rodents clearly limits the width of the active site channel in mouse and rat VAP-1. The residues that differ are shown as sticks; human (blue), monkey (green), rat (yellow) and mouse (magenta). C) Differences affecting the binding of inhibitor **13** in hVAP-1 compared with mouse VAP-1. (Figure adapted from Publication III, Figure 1 and Publication II, Figure 4.)

5.4 Evolution and functional classification of CAOs (IV)

5.4.1 General topology of the CAO phylogenetic tree (IV)

Phylogenetic trees were inferred using MEGA5, with ML and NJ methods. In total, 245 sequences from 78 species were used for the analysis. The ML and NJ trees are congruent, showing 3 distinct branches with bootstrap support ranging from 93% to 99% (Figure 12). Each of the three branches contain a different member of the CAO family with DAO proteins grouped in one branch, RAO proteins in another branch and VAP-1 and SAO proteins grouped together in the same branch. VAP-1 and SAO group together due to their high sequence identity of 84 to 92%. The branch lengths in Figure 12 are scaled to show relative evolutionary distance. The distances of the three branches show that RAO and VAP-1/SAO proteins are more closely related, while DAO presents a larger evolutionary distance to the rest of the proteins. The 3D multivariate plot generated is also congruent with the phylogenetic tree of the CAOs (Figure 12B).
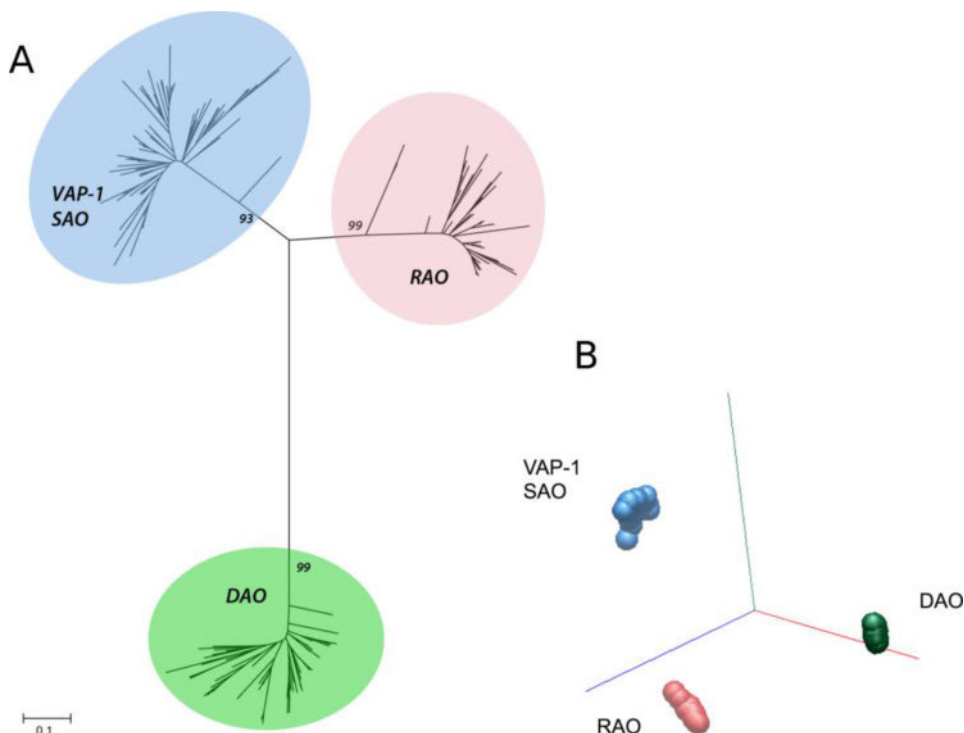
Figure 12. Phylogenetic analysis of the CAOs. A) Maximum Likelihood tree based on JTT matrix-based model. The tree is drawn to scale, with branch lengths measured in the number of substitutions per site. Bootstrap values are shown to each main branch. B) Multivariate plot reflect the data for the phylogenetic tree. (Publication IV, Figure 2)

5.4.2 New insights into the classification of CAOs (IV)

CAOs have a highly conserved motif in the active site: Thr/Ser-X1-X2-Asn-Tyr-Asp/Glu (Klinman, 1996). Based on the phylogenetic tree, protein sequences in the DAO branch have Tyr in position X2, protein sequences in the RAO branch have Gly and protein sequences in the VAP-1 and SAO clade have a Leu in the corresponding X2 position (Table 3). Furthermore, analysis of the gene and sequence information of the VAP-1 and SAO proteins show that there is a clear division among the proteins in the VAP-1/SAO clade based on their residue in position X1. The proteins have either a Leu or a Met in position X1 and the two groups are actually coming from different genes (Figure 13). A multiple sequence alignment and phylogenetic trees with the proteins with Leu in position X1 marked as VAP-1 (AOC3) and proteins with Met in position X1 marked as SAO (AOC4) shows a clear divergence between the AOC3 and the

41

AOC4 gene product. Even though there is a clear division in the majority of the VAP-1 and SAO proteins, some SAO proteins (from dog, panda, water buffalo, cattle and bison) group together with VAP-1 in the multivariate 3D plot (Figure 13B).

Table 3. The active site motif in the different CAOs.

	Thr/Ser	X1	X2	Asn	TPQ	Asp
DAO	Thr	Val	Tyr	Asn	Tyr	Asp
RAO	Ser	Val	Gly	Asn	Tyr	Asp
VAP-1	Thr	Leu	Leu	Asn	Tyr	Asp
SAO	Thr	Met	Leu	Asn	Tyr	Asp
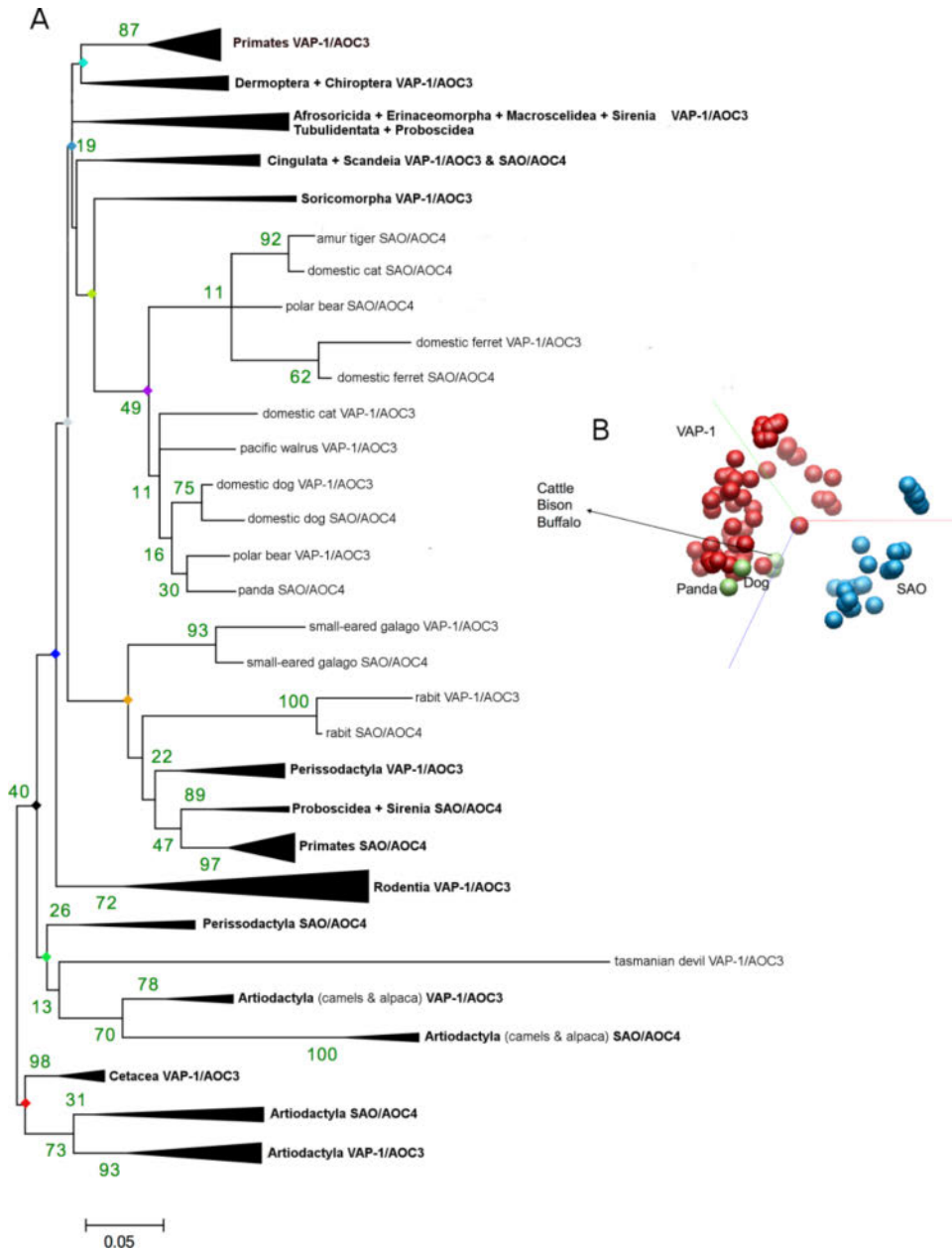
Figure 13. Phylogenetic analyses of VAP-1 and SAO proteins. A) The phylogenetic tree is inferred using Maximum Likelihood method based on the JTT matrix-based model. The tree is drawn to scale, with branch lengths measured in the number of substitutions per site. Last common ancestor marked with diamond. Bootstrap values are displayed in green. B) The multivariate plot confirms the division of VAP-1 and SAO proteins. (Publication IV, Figure 5)

5.5 VAP-1 to RAO mutations (I, IV)

The phylogenetic study confirmed that the CAOs can be classified based on the residues in the conserved active site motif, and that the residue in position X2 can be used to discriminate between the different CAOs (Table 3 & Figure 14). The active site close to TPQ is highly conserved. It is known that the CAOs have differences in their substrate preferences and the residue in position X2 is one of the reasons for the differences in substrate specificity. By experimentally mutating four residues in the VAP-1 active site to the corresponding ones in RAO (Met211Val, Thr212Ala, Tyr394Asn, and Leu469Gly) we could show that VAP-1 gets the substrate preferences of RAO. The mutations Leu469Gly and Met211Val especially affect the shape and size of the cavities. Leu469Gly mutation has the largest effect on the enzymatic properties and increases the oxidation of benzylamine (BZ) and 2-phenylethylamine (PEA) about 10-fold. In addition, the Leu469Gly mutant protein is able to oxidize p-tyramine (TYR) in contrast to WT VAP-1. The Met211Val mutation causes the active site to connect to the water channel instead of the active site channel. The mutational studies provide insight to the active site and function of RAO until a crystal structure is determined.
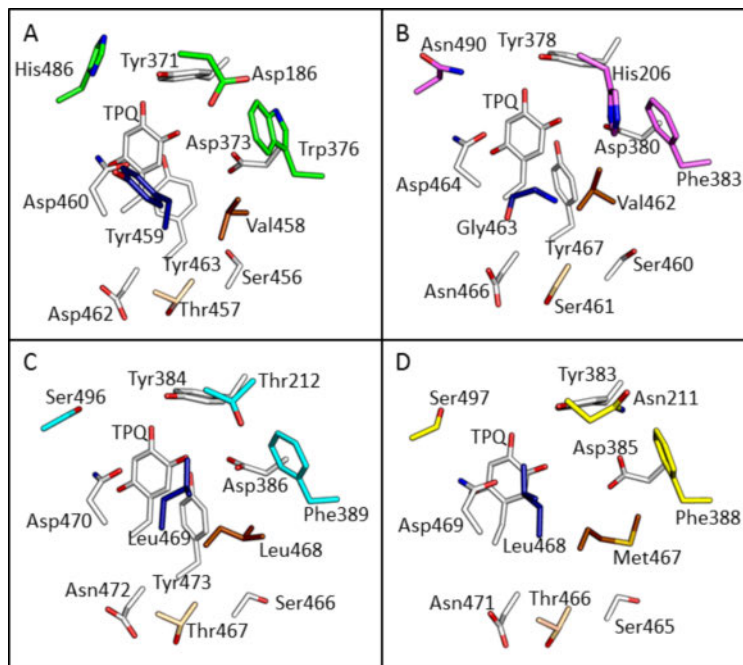
Figure 14. The CAO active sites with TPQ. Residues that are conserved in all CAOs are shown in white and non-conserved but similar residues are shown in light orange. A) DAO residues are shown in green. B) RAO residues are shown in pink. C) VAP-1 residues are shown in blue. D) SAO residues are shown in yellow. The conserved active site motif can be used as a basis for classification of the CAOs. Residues in position X1 in the active site motif are shown in brown and residues in position X2 are shown in dark blue. (Publication IV, Figure 6)

6. DISCUSSION

Currently there is a need for development of new types of medication against inflammatory and vascular diseases in the world. The amine oxidase involvement in human pathophysiological conditions has been known for decades (Boomsma et al., 2003) and its potential as a drug target in inflammatory diseases was noted shortly after the cloning and characterization of VAP-1 (Smith et al., 1998). As VAP-1 is involved in leukocyte transmigration to sites of inflammation it is possible to alleviate inflammatory conditions by blocking the adhesive and enzymatic function of VAP-1. VAP-1 is, therefore, a promising drug target. The results of these studies revealed a new mode of VAP-1 inhibition and molecular information important to the field of CAO research.

6.1 VAP-1, a challenging crystallographic target

In this study, five structures of hVAP-1 were determined by X-ray crystallography. The structures are overall similar to other reported CAO structures with a dimer as the biological unit and the monomer comprised of three domains (D2, D3 and D4), but they reveal new and interesting information. VAP-1 has proven to be a challenging crystallographic target with fragile and anisotropic crystals resulting in low-resolution structures. Before this study, there were only four crystal structures of mammalian CAOs available in complex with an inhibitor, hVAP−2HP complex (Jakobsson et al., 2005), bSAO in complex with clonidine (Holt et al., 2008), and DAO in complex with berenil and pentamidine (McGrath et al., 2009). Lunelli and coworkers have reported that deglycosylation was necessary to grow crystals of bSAO (Calderone et al., 2003). Here, we managed to grow crystals without deglycosylating the protein, but the crystals grew slowly, were anisotropic, extremely fragile and radiation-sensitive, which made the data collection challenging. The resolution of the new structures is between 2.60 and 3.10 Å, but the electron density is good throughout the structures. The $2F_o$-F_c maps together with the omit maps of the important regions clearly show the orientation of TPQ, the inhibitors and the side chain conformations of other important residues. For the inhibitor complex structures, corrections for anisotropy during data processing was especially important, as the effective resolution along the 6-fold axis was about 3.9 Å, while the effective resolution along the perpendicular directions was better than 3.0 Å.

Here we have determined the structure of cleaved human sVAP-1 for the first time, and two imidazole molecules from the crystallization buffer were bound in the protein. The sVAP-1 structures demonstrate the flexibility of TPQ, which was found in two different conformations, active off-copper and inactive on-copper, even though the crystals were grown in similar conditions. In the inactive on-copper TPQ conformation, imidazole makes a hydrogen bond to TPQ similarly as the imidazole in the active site of *Pichia Pastoris* CAO (PDB code 1RKY) (Duff et al., 2004) and (PDB code 1W7C) (Duff et al., 2006) and the imidazolidine ring of clonidine in the bSAO structure (Holt et al., 2008) (Figure S5 in Supporting Information in I). The other structure, where the TPQ is in active off-copper conformation and covalently bound to the imidazole, shows resemblance to the hVAP-1-2HP-complex (PDB code 2C11) (Jakobsson et al., 2005) (Figure S5 in Supporting Information in I).

6.2 Secondary imidazole binding site

It was experimentally shown that a 100 mM concentration of imidazole inhibits 93% of the VAP-1 activity. In addition to the TPQ-bound imidazole the sVAP-1 structures revealed a second imidazole binding site in the active site channel. The second imidazole molecule bound in the channel is hydrogen bonding to Thr212 and Tyr394. This secondary imidazole binding site in hVAP-1 seems to be different from the allosteric imidazoline binding site suggested for bSAO by kinetic studies performed by Holt and coworkers (Holt et al., 2008), because the corresponding residue to Tyr394 is Phe393 in bSAO, and Phe lacks the hydroxyl group of Tyr that binds the second imidazole molecule. With the help of the new sVAP-1 structures, the previously published VAP-1 structure (PDB code 1US1) (Airenne et al., 2005) could be re-evaluated and it turned out that an imidazole molecule can be built close to the TPQ. The imidazole bound in the active site channel disproves the prediction that Thr212 would be O-glycosylated (Airenne et al., 2005). These results, and the fact that an inhibitory effect of imidazole has previously been reported (Kelly et al., 1981), show the importance of excluding imidazole from the crystallization setup of CAO-inhibitor complexes.

6.3 VAP-1 old target, new inhibition mode

After the discovery of the secondary imidazole binding site in the active site channel, the idea of targeting the channel with small molecular inhibitors was raised. The majority of the earlier inhibitors for VAP-1 have been suicide

inhibitors like 2HP, which bind covalently to TPQ. Irreversible binding is not a desirable characteristic for a drug for human use (Palfreyman et al., 1994). A drug for human use should be removable, and the target activity should be regained within a short period of time. Therefore, a novel set of pyridazinone inhibitors targeted to the active site channel were designed and synthesized. The inhibitors showed great potency against hVAP-1 (IC_{50} values of 26-250 nM), and they were also specific for hVAP-1 over MAOs and DAO. During the recent years the idea of reversible inhibitors for CAOs has evolved and BSAO and hDAO have been crystallized together with reversible inhibitors (Holt et al., 2008; McGrath et al., 2009).

The crystal structure of the VAP-1 inhibitor complexes showed that the inhibitors **6**, **7** and **13** successfully bind noncovalently in the active site channel close to the secondary imidazole binding site, which is completely different from the complex structure of hVAP-1 and 2HP (Jakobsson et al., 2005). The binding of the inhibitors do not cause any major changes in the conformation of the residues in the active site channel compared to the native structure of VAP-1, except for Phe173 that has taken an alternative conformation to allow passage and create additional space for the inhibitors to bind. The phenyl ring of Phe389 has also rotated to make more favorable interactions to inhibitors **6** and **7**. The binding of these inhibitors block the entrance and hinder any ligand of entering the active site.

Similarly, like the second imidazole molecule in VAP-1, clonidine in bSAO (Lunelli et al., 2005), berenil and pentamidine (McGrath et al., 2009) inhibitors bind noncovalently to DAO, but superposition of the structures show that the pyridazinone inhibitors bind further out in the active site channel than the other inhibitors (Figure 3 in I). The closest point of contact to TPQ in the berenil-hDAO complex is 4.5 Å, in the pentamidine-hDAO complex it is 4.0 Å, in the pyridazinone-VAP-1 complexes the distance to TPQ is 6.1-6.9 Å, while the secondary imidazole binding site lays 10 Å from TPQ (Figure 3 in I & Figure 9F). Arm I from the other monomer makes the entrance to the active site channel narrower in DAO than in VAP-1, which might affect the ligand binding properties (Figure 3 in I). The matter of reversible inhibitors for VAP-1 has subsequently been discussed by Bonaiuto and coworkers who recognized a synthetic polyamine as a reversible inhibitor that binds in the active site channel and blocks the entrance to TPQ (Bonaiuto et al., 2012), similarly to the pyridazinone inhibitors. The binding mode for the pyridazinone inhibitors is

also different from other recent computational studies, where docking and QSAR models of potential VAP-1 inhibitors have been published (Foot et al., 2012; Inoue et al., 2013a; Inoue et al., 2013b; Nurminen et al., 2010; Nurminen et al., 2011).

6.3.1 Molecular binding mode of the pyridazinone inhibitors

Due to the scaffold, the inhibitors show a similar binding mode with only minor differences in their hydrogen bonds, π-stacking, and hydrophobic interactions to VAP-1. There are hydrophobic interactions by Phe173, Leu177, Leu468, and Leu469 to the inhibitors. It has been shown that the enzyme substrate recognition step in VAP-1 is mainly controlled by hydrophobic interactions (Bonaiuto et al., 2010) and actually, the largest and most hydrophobic inhibitor, **13**, shows the best binding. The second phenyl ring and the piperazine group of **13** accounts for its better binding because the lack of these groups in inhibitor **7** leads to lower potency. Arm I from the other monomer is apparently important for the binding of the inhibitors as Tyr448B makes a hydrogen bond with all inhibitors.

The side chain of Thr212 is flexible and makes a water mediated hydrogen bond to the inhibitors in all A chains and in the other chains it is not interacting with the inhibitors but is hydrogen bonded to Arg216. However, Thr212 is also involved in the binding of the second imidazole, and the corresponding residue Asp186 in DAO has been shown to bind the second amine of the diamine substrates (McGrath et al., 2009), and therefore, this position seems to be of special importance in ligand binding. Actually, the only substitution between the cynomolgus monkey and the human is this residue. However, the substitution Thr212[human]/Asn[monkey] does not cause any difference in the binding of the inhibitors, as the inhibitors bind both proteins equally well because Asn212[monkey] can interact with the inhibitors.

6.3.2 Species specific binding of the pyridazinone inhibitors

Even though **6**, **7**, and **13** are potent hVAP-1 inhibitors, they are surprisingly weak inhibitors of mouse VAP-1 activity. In our attempts to explain the species-specific binding properties of the pyridazinone inhibitors, we made homology models of monkey, mouse and rat VAP-1 based on the crystal structure of hVAP-1. Based on the models we could not find any prominent differences between the rodent and primate VAP-1 in the active site near TPQ. Marti and

coworkers could not either find any differences close to TPQ in their previous homology models of the mouse VAP-1 (Marti et al., 2004). This is in line with the experimental results from this study, as the activity measurements with the control compound, a hydrazine derived inhibitor (Nurminen et al., 2011) which binds to TPQ, inhibits both rodent and primate VAP-1. However, when we extended the analysis to the active site channel and the region where the second imidazole and the inhibitors bind, we could find significant differences.

From the comparison of the active site shape in primate and rodent VAP-1 it was seen that the active site of rodent VAP-1 is narrower than the active site in primates. Especially, the substitution of Leu447B/Phe[rat/mouse] in Arm I, which reaches the active site channel from the other monomer, clearly restricts the width of the channel and the space for the inhibitors. It is thought that Arm I, is important for the dimer stability and regulation of substrate specificity in the CAOs (Klema & Wilmot, 2012). Here we can clearly see that the substitution of a smaller Leu in the primate VAP-1 to a larger Phe in the rodents is important for the ligand to access the active site, and therefore, we suggest that this residue can function as a porter residue in the rodent VAP-1. This suggestion is supported by the fact that Inoue and coworkers also identified the Leu447B/Phe[rat] substitution to cause species specific binding differences of their thiazole derivative inhibitors, which bind TPQ but due to their size extends out to the active site channel (Inoue et al., 2013a; Inoue et al., 2013b).

Based on our modelled mouse VAP-1 there are, in addition to the shape differences of the active sites, less favorable interactions between the mouse VAP-1 and inhibitor **13** than with hVAP-1. These differences can explain the poor inhibitor potency against the mouse VAP-1. The Phe173/Asp[mouse] substitution together with His762/Tyr[mouse] affects inhibitor binding, as the interaction between Asp and Tyr in the mouse VAP-1 restricts the entrance to the active site. In hVAP-1 Tyr448B and Asp180 are both involved in hydrogen bonding to the inhibitor, while in mouse VAP-1, these interactions are missing. The active site channel of hVAP-1 is more hydrophobic than mouse VAP-1 because of Phe173/Asp[mouse] and Leu177/Gln[mouse] substitutions in which hydrophobic residues are changed to a charged and a polar residue in the mouse protein. As the pyridazinone inhibitors are rather large and hydrophobic, the interactions are not as favorable in the mouse VAP-1 as in the hVAP-1.

6.4 The evolution of CAOs

The phylogenetic tree of the CAOs contains three major branches. The distances of the three branches show that RAO, VAP-1, and SAO, proteins are more closely related, while DAO presents a larger evolutionary distance to the rest of the proteins. The distances also show that VAP-1 and SAO proteins are the closest relatives of the CAOs, and that they seem to have diverged more recently than RAO and DAO. The multivariate analysis confirms these results, as the proteins cluster together in a similar way in the 3D plots. The 3D multivariate analysis represents a nice support and validation tool for the phylogenetic studies, as the plot shows the relation of the individual clusters. It is not surprising that DAO is most distantly related in the CAO family, because the DAO encoding gene, AOC1, is not linked to the other genes (Schwelberger, 2010).

6.4.1 Classification of CAOs, VAP-1 and SAO

CAOs are currently classified into EC 1.4.3.21 (RAO, VAP-1, SAO) and EC 1.4.3.22 (DAO) families. The results from the phylogenetic study of the large set of CAO sequences show the importance of the Thr/Ser-X1-X2-Asn-Tyr-Asp/Glu active site motif and confirm that positions X1 and X2 could be used to classify CAOs into AOC1-4 sub families. Based on the phylogenetic tree, all protein sequences in the DAO branch have Tyr in position X2, all protein sequences in the RAO branch have Gly, and all protein sequences in the VAP-1 and SAO clade have a Leu in the corresponding X2 position. Therefore, the results support the idea that the residue in position X2 can be used as criteria to differentiate between mammalian CAO proteins. Even though the mammalian CAOs can easily be classified based on the residue in position X2 of the active site motif, a correct and formal method to distinguish between VAP-1 and SAO proteins has been missing and the majority of SAO proteins is annotated as membrane primary amine oxidase-like. Here we found a clear division among the proteins in the VAP-1/SAO clade based on their residue in the position X1. Sequence alignment and the phylogenetic tree reveal that VAP-1 proteins have a Leu in position X1, while SAO proteins have a Met in position X1 in the active site motif, and therefore, we suggest that VAP-1 and SAO can be classified based on the residue in position X1.

Regarding the closely related VAP-1 and SAO, it seems that they have evolved differently in individual species due to varying evolutionary pressure. In some

species, the SAO proteins seems to be the ancestral protein and duplication has given origin to VAP-1 (rabbit and lemur), while in other species, it is the opposite with VAP-1 giving origin to SAO (nine-banded armadillo and chinese tree shrew). It also varies among the species when the divergence between VAP-1 and SAO occurred, and not all species have both VAP-1 and SAO proteins. It is possible that the mutation that gave origin to the stop codon in human SAO was favored because the soluble form of VAP-1 (sVAP-1) can substitute SAO. In dog, the SAO protein is an isoform from the AOC3 gene, while in panda the sequence is from the AOC3 gene but contains a Met in position X1 that according to the classification rules makes it VAP-1. It might, however, be that the divergence between VAP-1 and SAO into two distinct proteins is still occurring in the dog and the bovine, which represents outliers in the study. The mutation that causes the change from Leu to Met, and makes the difference between VAP-1 and SAO, is only one base pair in the codon. Moreover, dog VAP-1 and SAO proteins might give important insight into the evolution of the proteins, as there is positive selection for both isoforms from the same gene.

6.5 VAP-1 to RAO mutations

Kaitaniemi and coworkers have previously shown that a triple mutant (Mel211Val/Tyr394Asn/Leu469Gly) of VAP-1 where the three residues in the active site are changed to the corresponding ones in RAO affect the substrate preference profile (Kaitaniemi et al 2009). In this study, these residues and Thr212 were individually mutated and the results showed that Leu469 and Met211 are important for VAP-1 substrate recognition. The absence of the gate residue Leu469 (Airenne et al 2005, Jakobsson et al 2005, Lunelli et al 2005) in the Leu469/Gly mutation together with the Thr212Ala and Met211Val mutations makes the active site channel more open and the substrates can easily reach and bind TPQ (Figure 7B in I), hence the improved oxidation of BZ and PEA. However, it seems that loss of Met211 and hydrophobic side chains makes the correct positioning of the small methylamine (MA) difficult. Met211 and Leu469 have previously been reported flexible and in different conformations (Figure 8 in I) (Lunelli et al., 2005; McGrath et al., 2009; Nurminen et al 2010), which supports the idea that they are important in substrate acceptance, preference and/or positioning. Met211Val also cause changes in the active site channel so that the primary active site is connected to a water channel instead of the active site channel.

7. CONCLUSIONS

In summary, these results will altogether aid future development and design of therapeutics for inflammatory diseases, and especially, VAP-1-associated diseases. The identification of a secondary binding site in the active site channel, together with the detailed binding mode revealed by crystal structures of the novel pyridazinone inhibitors, will further enable the development of new type of pyridazinone inhibitors, as well as, other completely different reversible inhibitors. Anti-VAP-1 antibodies might be closer to the market, but the small molecular inhibitors compose an attractive alternative as they can simultaneously inhibit the adhesive and enzymatic activity of VAP-1 and, therefore, inhibit both the transmigration of leukocytes and the proinflammatory effects of VAP-1 activity.

The new structural information of the VAP-1 active site, provided by X-ray structures and homology models, is of importance in drug design. The active site of enzymes and their known ligands can be utilized as a starting point for rational drug design, as analogues of known substrates and inhibitors can be designed and developed (Salmi & Jalkanen, 2005). Available crystal structures will not only aid in the planning and development of new inhibitors, but will also aid in the development of PET-tracers and other diagnostic tools.

The results of this study also draw attention to the importance of acknowledging species specific differences in the drug development. Here we have clear differences in the binding of the pyridazinone inhibitors to the rodent and primate proteins. As rodents are often used for *in vivo* testing of candidate drugs, it is especially important to acknowledge, that there can be small but crucial species specific differences in the proteins even though the sequence identity is rather high.

The results from the phylogenetic study confirm that the CAOs can be classified based on their residue in position X2 in the Thr/Ser-X1-X2-Asn-Tyr-Asp/Glu active site motif. We could also confirm that the VAP-1 and SAO sequences can be distinguished by the residue in position X1. These results will aid in the classification of new CAO sequences, and also in the reclassification of wrongly annotated sequences.

8. FUTURE PERSPECTIVES

The results from this study will be of use in the development of new and improved drugs in inflammatory diseases. One way to follow up on this study would be to improve the rodent VAP-1 inhibition of the pyridazinone inhibitors. However, the excellent specificity for hVAP-1 would need to be contained and that seems challenging, because the residues differing between the rodent and the primate protein are well-distributed in the active site channel. The differences affect the binding of several functional groups of the inhibitors. As there are significant differences between the species throughout the binding site in the active site channel, it is likely that specificity for the human protein is lost if the specificity for the rodent protein is improved. Other modifications to the inhibitors could also increase their promiscuity for other CAOs or even introduce toxicological liabilities that comprise their further development. Therefore, it is suggested that the species specific binding properties of these pyridazinone inhibitors are acknowledged and other methods than *in vivo* rodent testing are worth considering for future studies. Suitable approaches could include the use of human *in vivo* transgenic mice models, and other *in vitro* or *ex vivo* human disease-models. Nonhuman primate disease models can be used for toxicological and efficacy studies where suitable models exist and new human disease models could be developed (Peltz, 2013; Misharin et al., 2010; Imam et al., 2013).

The understanding of VAP-1 and its molecular mechanisms and functionalities are highly desirable as VAP-1 is such a promising drug target in inflammatory diseases. Further characterization of the VAP-1 counter-receptors Siglec-9 and Siglec-10, will reveal more information about their interaction with VAP-1. The determination of the precise interaction site and mode will help to improve existing VAP-1 inhibitors and aid in the planning of new inhibitors. We studied the evolution of the different CAOs and the next step would be to do a protein specific phylogenetic study, to analyze how the different proteins have evolved in different organisms and to pinpoint species specific differences that could be involved in substrate recognition and binding.

9. REFERENCES

Aalto, K., Autio, A., Kiss, E. A., Elima, K., Nymalm, Y., Veres, T. Z., Marttila-Ichihara, F., Elovaara, H., Saanijoki, T., Crocker, P. R., Maksimow, M., Bligt, E., Salminen, T. A., Salmi, M., Roivainen, A., & Jalkanen, S. (2011) Siglec-9 is a novel leukocyte ligand for vascular adhesion protein-1 and can be used in PET imaging of inflammation and cancer. *Blood, 118*(13), 3725-3733

Aalto, K., Maksimow, M., Juonala, M., Viikari, J., Jula, A., Kähönen, M., Jalkanen, S., Raitakari, O. T, & Salmi, M. (2012) Soluble vascular adhesion protein-1 correlates with cardiovascular risk factors and early atherosclerotic manifestations. *Arteriosclerosis, Thrombosis, and Vascular Biology, 32*(2), 523-532

Abella, A., Garcia-Vicente, S., Viguerie, N., Ros-Baro, A., Camps, M., Palacin, M., Zorzano, A., & Marti, L. (2004) Adipocytes release a soluble form of VAP-1/SSAO by a metalloprotease-dependent process and in a regulated manner. *Diabetologia, 47*(3), 429-438

Adams, P. D., Afonine, P. V., Bunkoczi, G., Chen, V. B., Davis, I. W., Echols, N., Headd J., Hung, L., Kapral, G., Grosse-Kunstleve, R., McCoy, A., Moriarty, N., Oeffner, R., Read, R., Richardson, D., Richardson, J., Terwilliger, T., Zwart, P. H. (2010) PHENIX: A comprehensive python-based system for macromolecular structure solution. *Acta Crystallographica Section D, Biological Crystallography, 66*(Pt 2), 213-221

Airas, L., Mikkola, J., Vainio, J. M., Elovaara, I., & Smith, D. J. (2006) Elevated serum soluble vascular adhesion protein-1 (VAP-1) in patients with active relapsing remitting multiple sclerosis. *Journal of Neuroimmunology, 177*(1-2), 132-135

Airenne, T. T., Nymalm, Y., Kidron, H., Smith, D. J., Pihlavisto, M., Salmi, M., Jalkanen, S., Johnson, M. S., & Salminen, T. A. (2005) Crystal structure of the human vascular adhesion protein-1: Unique structural features with functional implications. *Protein Science : A Publication of the Protein Society, 14*(8), 1964-1974

Altschul, S. F., Gish, W., Miller, W., Myers, E. W., & Lipman, D. J. (1990) Basic local alignment search tool. *Journal of Molecular Biology, 215*(3), 403-410

Autio, A., Vainio, P. J., Suilamo, S., Mali, A., Vainio, J., Saanijoki, T., Noponen, T., Ahtinen, H., Luoto, P., Teräs, M., Jalkanen, S., & Roivainen, A. (2013) Preclinical evaluation of a radioiodinated fully human antibody for in vivo imaging of vascular adhesion protein-1-positive vasculature in inflammation. *Journal of Nuclear Medicine: Official Publication, Society of Nuclear Medicine, 54*(8), 1315-1319

Bligt-Linden, E., Pihlavisto, M., Szatmari, I., Otwinowski, Z., Smith, D. J., Lazar, L., Fulop, F., & Salminen, T. A. (2013) Novel pyridazinone inhibitors for vascular

adhesion protein-1 (VAP-1): Old target-new inhibition mode. *Journal of Medicinal Chemistry, 56*(24), 9837-9848

Bonaiuto, E., Lunelli, M., Scarpa, M., Vettor, R., Milan, G., & Di Paolo, M. L. (2010) A structure-activity study to identify novel and efficient substrates of the human semicarbazide-sensitive amine oxidase/VAP-1 enzyme. *Biochimie, 92*(7), 858-868

Bonaiuto, E., Minarini, A., Tumiatti, V., Milelli, A., Lunelli, M., Pegoraro, M., Rizzoli, V., & Di Paolo, M. L. (2012) Synthetic polyamines as potential amine oxidase inhibitors: A preliminary study. *Amino Acids 42*(2-3), 913-28.

Bonder, C. S., Norman, M. U., Swain, M. G., Zbytnuik, L. D., Yamanouchi, J., Santamaria, P., Ajuebor, M., Salmi, M., Jalkanen, S., & Kubes, P. (2005) Rules of recruitment for Th1 and Th2 lymphocytes in inflamed liver: A role for alpha-4 integrin and vascular adhesion protein-1. *Immunity, 23*(2), 153-163

Boomsma, F., Bhaggoe, U. M., van der Houwen, A. M., & van den Meiracker, A. H. (2003) Plasma semicarbazide-sensitive amine oxidase in human (patho)physiology. *Biochimica Et Biophysica Acta, 1647*(1-2), 48-54

Boomsma, F., van Veldhuisen, D. J., de Kam, P. J., Man in't Veld, A. J., Mosterd, A., Lie, K. I., & Schalekamp, M. A. (1997) Plasma semicarbazide-sensitive amine oxidase is elevated in patients with congestive heart failure. *Cardiovascular Research, 33*(2), 387-391

Borek, D., Cymborowski, M., Machius, M., Minor, W., & Otwinowski, Z. (2010) Diffraction data analysis in the presence of radiation damage. *Acta Crystallographica Section D, Biological Crystallography, 66*(Pt 4), 426-436

Borek, D., Dauter, Z., & Otwinowski, Z. (2013) Identification of patterns in diffraction intensities affected by radiation exposure. *Journal of Synchrotron Radiation, 20*(Pt 1), 37-48

Borek, D., Minor, W., & Otwinowski, Z. (2003) Measurement errors and their consequences in protein crystallography. *Acta Crystallographica.Section D, Biological Crystallography, 59*(Pt 11), 2031-2038

Buffoni, F. (1966) Histaminase and related amine oxidases. *Pharmacological Reviews, 18*(4), 1163-1199

Calderone, V., Di Paolo, M. L., Trabucco, M., Biadene, M., Battistutta, R., Rigo, A., & Zanotti, G. (2003) Crystallization and preliminary X-ray data of amine oxidase from bovine serum. *Acta Crystallographica Section D, Biological Crystallography, 59*(Pt 4), 727-729

Chen, K., Maley, J., & Yu, P. H. (2006) Potential inplications of endogenous aldehydes in beta-amyloid misfolding, oligomerization and fibrillogenesis. *Journal of Neurochemistry, 99*(5), 1413-1424

Davis, I. W., Leaver-Fay, A., Chen, V. B., Block, J. N., Kapral, G. J., Wang, X., Murray, L., Arendall, B., Snoeyink, J., Richardson, J. S. & Richardson, D. C. (2007) MolProbity: All-atom contacts and structure validation for proteins and nucleic acids. *Nucleic Acids Research, 35*, W375-83

DeLano, W. L. (2008) The PyMoL molecular graphics systems. *Scientific LLC: Palo Alto, CA, 2008*

Di Paolo, M. L., Stevanato, R., Corazza, A., Vianello, F., Lunelli, L., Scarpa, M., & Rigo, A. (2003) Electrostatic compared with hydrophobic interactions between bovine serum amine oxidase and its substrates. *The Biochemical Journal, 371*(Pt 2), 549-556

Dodson, E. J., Winn, M., & Ralph, A. (1997) Collaborative computational project, number 4: Providing programs for protein crystallography. *Methods in Enzymology, 277*, 620-633

Duff, A. P., Cohen, A. E., Ellis, P. J., Hilmer, K., Langley, D. B., Dooley, D. M., Freeman, H., & Guss, J. M. (2006) The 1.23 angstrom structure of pichia pastoris lysyl oxidase reveals a lysine-lysine cross-link. *Acta Crystallographica Section D, Biological Crystallography, 62*(Pt 9), 1073-1084

Duff, A. P., Trambaiolo, D. M., Cohen, A. E., Ellis, P. J., Juda, G. A., Shepard, E. M., Langley, D. Dooley, D., Freeman, H. & Guss, J. M. (2004) Using xenon as a probe for dioxygen-binding sites in copper amine oxidases. *Journal of Molecular Biology, 344*(3), 599-607

Dunkel, J., Aguilar-Pimentel, J. A., Ollert, M., Fuchs, H., Gailus-Durner, V., de Angelis, M. H., Jalkanen, S., Salmi, M., & Veres, T. Z. (2014) Endothelial amine oxidase AOC3 transiently contributes to adaptive immune responses in the airways. *European Journal of Immunology, 44*(11), 3232-3239

Dunkel, P., Balogh, B., Meleddu, R., Maccioni, E., Gyires, K., & Matyus, P. (2011) Semicarbazide-sensitive amine oxidase/vascular adhesion protein-1: A patent survey. *Expert Opinion on Therapeutic Patents, 21*(9), 1453-1471

Dunkel, P., Gelain, A., Barlocco, D., Haider, N., Gyires, K., Sperlagh, B., Magyar, K., Maccioni, E., Fadda, A., & Matyus, P. (2008) Semicarbazide-sensitive amine oxidase/vascular adhesion protein 1: Recent developments concerning substrates and inhibitors of a promising therapeutic target. *Current Medicinal Chemistry, 15*(18), 1827-1839

Elmore, B. O., Bollinger, J. A., & Dooley, D. M. (2002) Human kidney diamine oxidase: Heterologous expression, purification, and characterization. *Journal of Biological Inorganic Chemistry, 7*(6), 565-579

Elovaara, H., Kidron, H., Parkash, V., Nymalm, Y., Bligt, E., Ollikka, P., Smith, D. J., Pihlavisto, M., Salmi, M., Jalkanen, S., & Salminen, T. A. (2011) Identification of two imidazole binding sites and key residues for substrate specificity in human primary amine oxidase AOC3. *Biochemistry, 50*(24), 5507-5520

Emsley, P., & Cowtan, K. (2004) Coot: Model-building tools for molecular graphics. *Acta Crystallographica.Section D, Biological Crystallography, 60*(Pt 12 Pt 1), 2126-2132

Ernberg, K., McGrath, A. P., Peat, T. S., Adams, T. E., Xiao, X., Pham, T., Newman, J., McDonald, I. A., Collyer, C. A., & Guss, J. M. (2010) A new crystal form of human vascular adhesion protein 1. *Acta Crystallographica.Section F, Structural Biology and Crystallization Communications, 66*(Pt 12), 1572-1578

Felsenstein J. (1985) Confidence limits on phylogenies: An approach using the bootstrap. *Evolution 39*(4), 783-791

Finney, J., Moon, H. J., Ronnebaum, T., Lantz, M., & Mure, M. (2014) Human copper-dependent amine oxidases. *Archives of Biochemistry and Biophysics, 546*, 19-32

Floris, G. (2009) Copper amine oxidases: Structures, catalytic mechanisms, and role in pathophysiology. *Boca Raton: CRC Press.*

Foot, J. S., Deodhar, M., Turner, C. I., Yin, P., van Dam, E. M., Silva, D. G., Olivieri, A., Holt, A., & McDonald, I. A. (2012) The discovery and development of selective 3-fluoro-4-aryloxyallylamine inhibitors of the amine oxidase activity of semicarbazide-sensitive amine oxidase/vascular adhesion protein-1 (SSAO/VAP-1). *Bioorganic & Medicinal Chemistry Letters, 22*(12), 3935-3940

Foot, J. S., Yow, T. T., Schilter, H., Buson, A., Deodhar, M., Findlay, A. D., Guo, L., McDonald, I. A., Turner, C. I., Zhou, W., & Jarolimek, W. (2013) PXS-4681A, a potent and selective mechanism-based inhibitor of SSAO/VAP-1 with anti-inflammatory effects in vivo. *The Journal of Pharmacology and Experimental Therapeutics, 347*(2), 365-374

Forster-Horvath, C., Dome, B., Paku, S., Ladanyi, A., Somlai, B., Jalkanen, S., & Timar, J. (2004) Loss of vascular adhesion protein-1 expression in intratumoral microvessels of human skin melanoma. *Melanoma Research, 14*(2), 135-140

Fowler, C., & Tipton, K. (1981) Concentration dependence of the oxidation of tyramine by the two forms of rat liver mitochondrial monoamine oxidase. *Biochemical Pharmacology 30*(24), 3329-3332

Garpenstrand, H., Ekblom, J., Backlund, L. B., Oreland, L., & Rosenqvist, U. (1999) Elevated plasma semicarbazide-sensitive amine oxidase (SSAO) activity in type 2 diabetes mellitus complicated by retinopathy. *Diabetic Medicine: A Journal of the British Diabetic Association, 16*(6), 514-521

Gokturk, C., Nilsson, J., Nordquist, J., Kristensson, M., Svensson, K., Soderberg, C., Israelsson, M., Garpenstrand, H., Sjoqvist, M., Oreland, L., & Forsberg-Nilsson, K. (2003) Overexpression of semicarbazide-sensitive amine oxidase in smooth muscle cells leads to an abnormal structure of the aortic elastic laminas. *The American Journal of Pathology, 163*(5), 1921-1928

Hartmann, C., & Klinman, J. P. (1991) Structure-function studies of substrate oxidation by bovine serum amine oxidase: Relationship to cofactor structure and mechanism. *Biochemistry, 30*(18), 4605-4611

Holt, A., Sharman, D. F., Baker, G. B., & Palcic, M. M. (1997) A continuous spectrophotometric assay for monoamine oxidase and related enzymes in tissue homogenates. *Analytical Biochemistry, 244*(2), 384-392

Holt, A., Smith, D. J., Cendron, L., Zanotti, G., Rigo, A., & Di Paolo, M. L. (2008) Multiple binding sites for substrates and modulators of semicarbazide-sensitive amine oxidases: Kinetic consequences. *Molecular Pharmacology, 73*(2), 525-538

Imam, S., Elagin, R. B., & Jaume, J. C. (2013) Diabetes-Associated Dry Eye Syndrome in a New Humanized Transgenic Model of Type 1 Diabetes. *Molecular Vision 8*(19), 1259-1267

Imamura, Y., Kubota, R., Wang, Y., Asakawa, S., Kudoh, J., Mashima, Y., Oguchi, Y., & Shimizu, N. (1997) Human retina-specific amine oxidase (RAO): cDNA cloning, tissue expression, and chromosomal mapping. *Genomics, 40*(2), 277-283

Inoue, T., Morita M., Tojo, T., Yoshihara, K., Nagashima, A., Moritomo, A., Ohkubo, M., & Miyake, H., (2013a) Synthesis and SAR study of new thiazole derivatives as vascular adhesion protein-1 (VAP-1) inhibitors for the treatment of diabetic macular edema. *Bioorganic & Medicinal Chemistry, 21*(5), 1219-1233

Inoue, T., Morita, M., Tojo, T., Nagashima, A., Moritomo, A., Imai, K., & Miyake, H. (2013b) Synthesis and SAR study of new thiazole derivatives as vascular adhesion protein-1 (VAP-1) inhibitors for the treatment of diabetic macular edema: Part 2. *Bioorganic & Medicinal Chemistry, 21*(9), 2478-2494

Irjala, H., Salmi, M., Alanen, K., Grenman, R., & Jalkanen, S. (2001) Vascular adhesion protein 1 mediates binding of immunotherapeutic effector cells to tumor endothelium. *Journal of Immunology, 166*(11), 6937-6943

Jaakkola, K., Nikula, T., Holopainen, R., Vahasilta, T., Matikainen, M. T., Laukkanen, M. L., Huupponen, R., Halkola, L., Nieminen, L., Hiltunen, J., Parviainen, S., Clark, M. R., Knuuti, J., Savunen, T., Kääpä, P., Voipio-Pulkki, L. M., & Jalkanen, S. (2000) In vivo detection of vascular adhesion protein-1 in experimental inflammation. *The American Journal of Pathology, 157*(2), 463-471

Jakobsson, E., Nilsson, J., Ogg, D., & Kleywegt, G. J. (2005) Structure of human semicarbazide-sensitive amine oxidase/vascular adhesion protein-1. *Acta Crystallographica.Section D, Biological Crystallography, 61*(Pt 11), 1550-1562

Jalkanen, S., Karikoski, M., Mercier, N., Koskinen, K., Henttinen, T., Elima, K., Salmivirta, K., & Salmi, M. (2007) The oxidase activity of vascular adhesion protein-1 (VAP-1) induces endothelial E- and P-selectins and leukocyte binding. *Blood, 110*(6), 1864-1870

Jalkanen, S., & Salmi, M. (2008) VAP-1 and CD73, endothelial cell surface enzymes in leukocyte extravasation. *Arteriosclerosis, Thrombosis, and Vascular Biology, 28*(1), 18-26

Jones, D. T., Taylor, W. R., & Thornton, J. M. (1992) The rapid generation of mutation data matrices from protein sequences. *Computer Applications in the Biosciences : CABIOS, 8*(3), 275-282

Kaitaniemi, S., Elovaara, H., Gron, K., Kidron, H., Liukkonen, J., Salminen, T., Salmi, M., Jalkanen, S., & Elima, K. (2009) The unique substrate specificity of human AOC2, a semicarbazide-sensitive amine oxidase. *Cellular and Molecular Life Sciences : CMLS, 66*(16), 2743-2757

Kelly, I. D., Knowles, P. F., Yadav, K. D., Bardsley, W. G., Leff, P., & Waight, R. D. (1981) Steady-state kinetic studies on benzylamine oxidase from pig plasma. *European Journal of Biochemistry / FEBS, 114*(1), 133-138

Kirton, C. M., Laukkanen, M. L., Nieminen, A., Merinen, M., Stolen, C. M., Armour, K., Smith, D. J., Salmi, M., Jalkanen, S., & Clark, M. R. (2005) Function-blocking antibodies to human vascular adhesion protein-1: A potential anti-inflammatory therapy. *European Journal of Immunology, 35*(11), 3119-3130

Kivi, E., Elima, K., Aalto, K., Nymalm, Y., Auvinen, K., Koivunen, E., Otto, D. M., Crocker, P. R., Salminen, T. A., Salmi, M., & Jalkanen, S. (2009) Human siglec-10 can bind to vascular adhesion protein-1 and serves as its substrate. *Blood, 114*(26), 5385-5392

Klema, V. J., & Wilmot, C. M. (2012) The role of protein crystallography in defining the mechanisms of biogenesis and catalysis in copper amine oxidase. *International Journal of Molecular Sciences, 13*(5), 5375-5405

Klinman, J. P. (1996) New quinocofactors in eukaryotes. *The Journal of Biological Chemistry, 271*(44), 27189-27192

Koskinen, K., Nevalainen, S., Karikoski, M., Hanninen, A., Jalkanen, S., & Salmi, M. (2007) VAP-1-deficient mice display defects in mucosal immunity and antimicrobial responses: Implications for antiadhesive applications. *Journal of Immunology, 179*(9), 6160-6168

Koskinen, K., Vainio, P. J., Smith, D. J., Pihlavisto, M., Yla-Herttuala, S., Jalkanen, S., & Salmi, M. (2004) Granulocyte transmigration through the endothelium is regulated by the oxidase activity of vascular adhesion protein-1 (VAP-1). *Blood, 103*(9), 3388-3395

Kabsch, W. (2010) XDS. *Acta Crystallographica Section D Biological Crystallography 66*(Pt 2), 125–132

Kurkijarvi, R., Adams, D. H., Leino, R., Mottonen, T., Jalkanen, S., & Salmi, M. (1998) Circulating form of human vascular adhesion protein-1 (VAP-1): Increased serum levels in inflammatory liver diseases. *Journal of Immunology (Baltimore, Md.: 1950), 161*(3), 1549-1557

Lalor, P. F., Edwards, S., McNab, G., Salmi, M., Jalkanen, S., & Adams, D. H. (2002) Vascular adhesion protein-1 mediates adhesion and transmigration of lymphocytes on human hepatic endothelial cells. *Journal of Immunology (Baltimore, Md.: 1950), 169*(2), 983-992

Lalor, P. F., Tuncer, C., Weston, C., Martin-Santos, A., Smith, D. J., & Adams, D. H. (2007) Vascular adhesion protein-1 as a potential therapeutic target in liver disease. *Annals of the New York Academy of Sciences, 1110*, 485-496

Laskowski, R. A. (1995) SURFNET: A program for visualizing molecular surfaces, cavities, and intermolecular interactions. *Journal of Molecular Graphics, 13*(5), 323-30, 307-8

Lehtonen, J. V., Still, D. J., Rantanen, V. V., Ekholm, J., Bjorklund, D., Iftikhar, Z., Huhtala, M., Repo, S., Jussila, A.,Jaakkola, J., Pentikäinen, O., Nyrönen, T., Salminen, A. T., Gyllenberg, M., & Johnson, M. S. (2004) BODIL: A molecular modeling environment for structure-function analysis and drug design. *Journal of Computer-Aided Molecular Design, 18*(6), 401-419

Li, H. Y., Wei, J. N., Lin, M. S., Smith, D. J., Vainio, J., Lin, C. H., Chiang, F., Shih, S., Huang, C., Wu, M., Hsein, Y., & Chuang, L. M. (2009a) Serum vascular adhesion protein-1 is increased in acute and chronic hyperglycemia. *Clinica Chimica Acta; International Journal of Clinical Chemistry, 404*(2), 149-153

Li, H. Y., Lin, M. S., Wei, J. N., Hung, C. S., Chiang, F. T., Lin, C. H., Hsu, H., Su, C., Wu, M., Smith, D., Vainio, J., Chen, M., & Chuang, L. M. (2009b) Change of serum vascular adhesion protein-1 after glucose loading correlates to carotid intima-medial thickness in non-diabetic subjects. *Clinica Chimica Acta; International Journal of Clinical Chemistry, 403*(1-2), 97-101Li, X.G., Autio A., Ahtinen H., Helariutta K., Liljenbäck H., Jalkanen S., Roivainen A., & Airaksinen A. J. (2013) Translating the concept of peptide labeling with 5-deoxy-5-[18F]fluororibose into preclinical practice: 18F-labeling of Siglec-9 peptide for PET imaging of inflammation. *Chemical Communication. 49(35), 3682-3684*

Li, Y. I., Hung, J. S., Yu, T. Y., Liou, J. M., Wei, J. N., Kao, H. L., Chaung, L., Shun, C., Lee, P., Su, C., Li, H., & Liang, J. T. (2014) Serum vascular adhesion protein-1 predicts all-cause mortality and cancer-related mortality in subjects with colorectal cancer. *Clinica Chimica Acta; International Journal of Clinical Chemistry, 428*, 51-56

Liaskou, E., Karikoski, M., Reynolds, G. M., Lalor, P. F., Weston, C. J., Pullen, N., Salmi, M., Jalkanen, S., & Adams, D. H. (2011) Regulation of mucosal addressin cell adhesion molecule 1 expression in human and mice by vascular adhesion protein 1 amine oxidase activity. *Hepatology (Baltimore, Md.), 53*(2), 661-672

Lin, M. S., Li, H. Y., Wei, J. N., Lin, C. H., Smith, D. J., Vainio, J., Shih, S., Chen, Y., Lin, L., Kao, H., Chuang, L., & Chen, M. F. (2008) Serum vascular adhesion protein-1 is higher in subjects with early stages of chronic kidney disease. *Clinical Biochemistry, 41*(16-17), 1362-1367

Lizcano, J. M., Fernandez de Arriba, A., Tipton, K. F., & Unzeta, M. (1996) Inhibition of bovine lung semicarbazide-sensitive amine oxidase (SSAO) by some hydrazine derivatives. *Biochemical Pharmacology, 52*(2), 187-195

Lucero, H. A., & Kagan, H. M. (2006) Lysyl oxidase: An oxidative enzyme and effector of cell function. *Cellular and Molecular Life Sciences : CMLS, 63*(19-20), 2304-2316

Lunelli, M., Di Paolo, M. L., Biadene, M., Calderone, V., Battistutta, R., Scarpa, M., Rigo, A., & Zanotti, G. (2005) Crystal structure of amine oxidase from bovine serum. *Journal of Molecular Biology, 346*(4), 991-1004

Luo, W., Xie, F., Zhang, Z., & Sun, D. (2013) Vascular adhesion protein 1 in the eye. *Journal of Ophthalmology, 2013*, 925267

Lyles, G. A. (1996) Mammalian plasma and tissue-bound semicarbazide-sensitive amine oxidases: Biochemical, pharmacological and toxicological aspects. *The International Journal of Biochemistry & Cell Biology, 28*(3), 259-274

Lyles, G. A., & Chalmers, J. (1992) The metabolism of aminoacetone to methylglyoxal by semicarbazide-sensitive amine oxidase in human umbilical artery. *Biochemical Pharmacology, 43*(7), 1409-1414

MacNee, W., Rabinovich, R., A., & Choudhury, G. (2014) Ageing and the border between health and disease. *European Respiratory Journal 44*(5), 1332-1352

Madej, A., Reich, A., Orda, A., & Szepietowski, J. C. (2007) Vascular adhesion protein-1 (VAP-1) is overexpressed in psoriatic patients. *Journal of the European Academy of Dermatology and Venereology : JEADV, 21*(1), 72-78

Maintz, L., & Novak, N. (2007) Histamine and histamine intolerance. *The American Journal of Clinical Nutrition, 85*(5), 1185-1196

Maintz, L., Schwarzer, V., Bieber, T., van der Ven, K., & Novak, N. (2008) Effects of histamine and diamine oxidase activities on pregnancy: A critical review. *Human Reproduction Update, 14*(5), 485-495

Martelius, T., Salaspuro, V., Salmi, M., Krogerus, L., Hockerstedt, K., Jalkanen, S., & Lautenschlager, I. (2004) Blockade of vascular adhesion protein-1 inhibits lymphocyte infiltration in rat liver allograft rejection. *The American Journal of Pathology, 165*(6), 1993-2001

Martelius, T., Salmi, M., Krogerus, L., Loginov, R., Schoultz, M., Karikoski, M., Miiluniemi, M., Soots, A., Höckerstedt, K., Jalkanen, S., & Lautenschlager, I. (2008) Inhibition of semicarbazide-sensitive amine oxidases decreases lymphocyte infiltration in the early phases of rat liver allograft rejection. *International Journal of Immunopathology and Pharmacology, 21*(4), 911-920

Marti, L., Abella, A., De La Cruz, X., Garcia-Vicente, S., Unzeta, M., Carpene, C., Palacin, M., Testar, X., Orozco, M., & Zorzano, A. (2004) Exploring the binding mode of semicarbazide-sensitive amine oxidase/VAP-1: Identification of novel substrates with insulin-like activity. *Journal of Medicinal Chemistry, 47*(20), 4865-4874

Marttila-Ichihara, F., Auvinen, K., Elima, K., Jalkanen, S., & Salmi, M. (2009) Vascular adhesion protein-1 enhances tumor growth by supporting recruitment of gr-1+CD11b+ myeloid cells into tumors. *Cancer Research, 69*(19), 7875-7883

Marttila-Ichihara, F., Smith, D. J., Stolen, C., Yegutkin, G. G., Elima, K., Mercier, N., Kiviranta, R., Pihlavisto, M., Alaranta, S., Pentikäinen, U., Pentikäinen, O., Fulop, F., Jalkanen, S., & Salmi, M. (2006) Vascular amine oxidases are needed for leukocyte extravasation into inflamed joints in vivo. *Arthritis and Rheumatism, 54*(9), 2852-2862

Maula, S. M., Salminen, T., Kaitaniemi, S., Nymalm, Y., Smith, D. J., & Jalkanen, S. (2005) Carbohydrates located on the top of the "cap" contribute to the adhesive and

enzymatic functions of vascular adhesion protein-1. *European Journal of Immunology, 35*(9), 2718-2727

McDonald, I. M., Foot, J., Yin, P., Flening, E., & van Dam, E., M. (2007) Semicarbazide sensitive amine oxidase and vacular adhesion protein-1: one protein being validated as a therapeutic target for inflammatory diseases. *Annual Reports in Medicinal Chemistry, 42*, 229-243

McGrath, A. P., Caradoc-Davies, T., Collyer, C. A., & Guss, J. M. (2010b) Correlation of active site metal content in human diamine oxidase with trihydroxyphenylalanine quinone cofactor biogenesis. *Biochemistry, 49*(38), 8316-8324

McGrath, A. P., Hilmer, K. M., Collyer, C. A., Dooley, D. M., & Guss, J. M. (2010a) A new crystal form of human diamine oxidase. *Acta Crystallographica.Section F, Structural Biology and Crystallization Communications, 66*(Pt 2), 137-142

McGrath, A. P., Hilmer, K. M., Collyer, C. A., Shepard, E. M., Elmore, B. O., Brown, D. E., Doodley, D. M., & Guss, J. M. (2009) Structure and inhibition of human diamine oxidase. *Biochemistry, 48*(41), 9810-9822

Merinen, M., Irjala, H., Salmi, M., Jaakkola, I., Hanninen, A., & Jalkanen, S. (2005) Vascular adhesion protein-1 is involved in both acute and chronic inflammation in the mouse. *The American Journal of Pathology, 166*(3), 793-800

Meyer, J. H., Ginovart, N., Boovariwala, A., Sagrati, S., Hussey, D., Garcia, A., Young, T., Praschak-Reider, N., Wilson, A. A., & Houle, S. (2006) Elevated monoamine oxidase a levels in the brain: An explanation for the monoamine imbalance of major depression. *Archives of General Psychiatry, 63*(11), 1209-1216

Misharin, A. V., Haines, G. K., Rose, S., Gierut, A. K., Hotchkiss, R. S., & Perlman, H. (2012) Development of a new humanized mouse model to study acute inflammatory arthritis. *Journal of Translational Medicine 10*(190)

Mure, M. (2004) Tyrosine-derived quinone cofactors. *Accounts of Chemical Research, 37*(2), 131-139

Mure, M., Mills, S. A., & Klinman, J. P. (2002) Catalytic mechanism of the topa quinone containing copper amine oxidases. *Biochemistry, 41*(30), 9269-9278

Murshudov, G. N., Vagin, A. A., & Dodson, E. J. (1997) Refinement of macromolecular structures by the maximum-likelihood method. *Acta Crystallographica Section D, Biological Crystallography, 53*(Pt 3), 240-255

Noda, K., Miyahara, S., Nakazawa, T., Almulki, L., Nakao, S., Hisatomi, T., She, H., Thomas, K. L., Garland, R. C., Miller, J. W., Gragoudas, E. S., Kawai, Y., Mashima,

Y., & Hafezi-Moghadam, A. (2008a) Inhibition of vascular adhesion protein-1 suppresses endotoxin-induced uveitis. *FASEB Journal, 22*(4), 1094-1103

Noda, K., She, H., Nakazawa, T., Hisatomi, T., Nakao, S., Almulki, L., Zandi, S., Miyahara, S., Ito, Y., Thomas, K. L., Garland, R. C., Miller, J. W., Gragoudas, E. S., Mashima, Y., & Hafezi-Moghadam, A. (2008b) Vascular adhesion protein-1 blockade suppresses choroidal neovascularization. *FASEB Journal 22*(8), 2928-2935

Noonan, T., Lukas, S., Peet, G. W., Pelletier, J., Panzenbeck, M., Hanidu, A., Mazurek, S., Wasti, R., Rybina, I., Roma, T., Kronkaitis, A., Shoultz, A., Souza, D., Jiang, H., Nabozny, G., & Modis, L. K. (2013) The oxidase activity of vascular adhesion protein-1 (VAP-1) is essential for function. *American Journal of Clinical and Experimental Immunology, 2*(2), 172-185

Nurminen, E. M., Pihlavisto, M., Lazar, L., Pentikainen, U., Fulop, F., & Pentikainen, O. T. (2011) Novel hydrazine molecules as tools to understand the flexibility of vascular adhesion protein-1 ligand-binding site: Toward more selective inhibitors. *Journal of Medicinal Chemistry, 54*(7), 2143-2154

Nurminen, E. M., Pihlavisto, M., Lazar, L., Szakonyi, Z., Pentikainen, U., Fulop, F., & Pentikainen, O. T. (2010) Synthesis, in vitro activity, and three-dimensional quantitative structure-activity relationship of novel hydrazine inhibitors of human vascular adhesion protein-1. *Journal of Medicinal Chemistry, 53*(17), 6301-6315

O'Rourke, A. M., Wang, E. Y., Miller, A., Podar, E. M., Scheyhing, K., Huang, L., Kessler, C., Gao, H., Ton-Nu, H., MacDonald, M. T., Jones, D. S., & Linnik, M. D. (2008) Anti-inflammatory effects of LJP 1586 [Z-3-fluoro-2-(4-methoxybenzyl)allylamine hydrochloride], an amine-based inhibitor of semicarbazide-sensitive amine oxidase activity. *The Journal of Pharmacology and Experimental Therapeutics, 324*(2), 867-875

O'Rourke, A. M., Wang, E. Y., Salter-Cid, L., Huang, L., Miller, A., Podar, E., Gao, H. F., Jones, D. S., & Linnik, M. D. (2007) Benefit of inhibiting SSAO in relapsing experimental autoimmune encephalomyelitis. *Journal of Neural Transmission, 114*(6), 845-849

Otwinowski, Z., & Minor, W. (1997) Processing of X-ray diffraction data collected in the oscillation mode. *Methods in Enzymology, 276*, 307-326

Palfreyman, M. G., McDonald, I. A., Bey, P., Danzin, C., Zreika, M., & Cremer, G. (1994) Haloallylamine inhibitors of MAO and SSAO and their therapeutic potential. *Journal of Neural Transmission.Supplementum, 41*, 407-414

Parsons M, r., Convery, M. A., Wilmot, C. M., Yadav, K. D. S., Blakeley, V., Corner, A. S., Philips, S. E. V., McPherson, M. J., & Knowles, P. F. (1995) Crystal structure of

quinoenzyme: copper amine oxidase of *Esterichia coli* at 2 Å resolution. *Structure 3*(11), 1171-1184

Peltz, G. (2013) Can 'Humanized' Mice Improve Drug Development in the 21st Century? *Trends in Pharmacological Sciences. 34*(5): 255–260

Roivainen, A., Jalkanen, S., & Nanni, C. (2012) Gallium-labelled peptides for imaging of inflammation. *European Journal of Nuclear Medicine and Molecular Imaging, 39 Suppl 1*, S68-77

Ruoslahti, E. & Pierschbacher, M.D. (1987) New perspectives in cell adhesion: RGD and integrins. *Science, 238*, 491-497

Sali, A., & Blundell, T. L. (1993) Comparative protein modelling by satisfaction of spatial restraints. *Journal of Molecular Biology, 234*(3), 779-815

Saitou, N., & Nei, M. (1987) The neighbor-joining method: A new method for reconstructing phylogenetic trees. *Molecular Biology and Evolution 4*, 406-425

Salmi, M., Hellman, J., & Jalkanen, S. (1998) The role of two distinct endothelial molecules, vascular adhesion protein-1 and peripheral lymph node addressin, in the binding of lymphocyte subsets to human lymph nodes. *Journal of Immunology, 160*(11), 5629-5636

Salmi, M., & Jalkanen, S. (1992) A 90-kilodalton endothelial cell molecule mediating lymphocyte binding in humans. *Science, 257*(5075), 1407-1409.

Salmi, M., Tohka, S., & Jalkanen, S. (2000) Human vascular adhesion protein-1 (VAP-1) plays a critical role in lymphocyte–endothelial cell adhesion cascade under shear stress. *Circulation Research 86*(12), 1245-1251

Salmi, M., & Jalkanen, S. (2001) VAP-1: An adhesin and an enzyme. *Trends in Immunology, 22*(4), 211-216

Salmi, M., & Jalkanen, S. (2005) Cell-surface enzymes in control of leukocyte trafficking. *Nature Reviews.Immunology, 5*(10), 760-771

Salmi, M., & Jalkanen, S. (2014) Ectoenzymes in leukocyte migration and their therapeutic potential. *Seminars in Immunopathology, 36*(2), 163-176

Salmi, M., Smith, D. J., Bono, P., Leu, T., Hellman, J., Matikainen, M. T., & Jalkanen, S. (1997) A mouse molecular mimic of human vascular adhesion protein-1. *Molecular Immunology, 34*(16-17), 1227-1236

Salmi, M., Stolen, C., Jousilahti, P., Yegutkin, G. G., Tapanainen, P., Janatuinen, T., Knip, M., Jalkanen, S., & Salomaa, V. (2002) Insulin-regulated increase of soluble

vascular adhesion protein-1 in diabetes. *The American Journal of Pathology, 161*(6), 2255-2262]

Salmi, M., Yegutkin, G. G., Lehvonen, R., Koskinen, K., Salminen, T., & Jalkanen, S. (2001) A cell surface amine oxidase directly controls lymphocyte migration. *Immunity, 14*(3), 265-276

Schwelberger, H. G. (2007) The origin of mammalian plasma amine oxidases. *Journal of Neural Transmission, 114*(6), 757-762

Schwelberger, H. G. (2010) Structural organization of mammalian copper-containing amine oxidase genes. *Inflammation Research, 59 Suppl 2,* S223-225

Seiler, N. (2004) Catabolism of polyamines. *Amino Acids, 26*(3), 217-233

Shih, J. C., Chen, K., & Ridd, M. J. (1999) Monoamine oxidase: From genes to behavior. *Annual Review of Neuroscience, 22*, 197-217

Smith, D. J., Salmi, M., Bono, P., Hellman, J., Leu, T., & Jalkanen, S. (1998) Cloning of vascular adhesion protein 1 reveals a novel multifunctional adhesion molecule. *The Journal of Experimental Medicine, 188*(1), 17-27

Smith, D. J., & Vainio, P. J. (2007) Targeting vascular adhesion protein-1 to treat autoimmune and inflammatory diseases. *Annals of the New York Academy of Sciences, 1110*, 382-388

Stolen, C. M., Marttila-Ichihara, F., Koskinen, K., Yegutkin, G. G., Turja, R., Bono, P., Skurnik, M., Hänninen, A., Jalkanen, S., & Salmi, M. (2005) Absence of the endothelial oxidase AOC3 leads to abnormal leukocyte traffic in vivo. *Immunity, 22*(1), 105-115

Su, Q., & Klinman, J. P. (1998) Probing the mechanism of proton coupled electron transfer to dioxygen: The oxidative half-reaction of bovine serum amine oxidase. *Biochemistry, 37*(36), 12513-12525

UniProt Consortium. (2015) UniProt: a hub for protein information. *Nucleic Acids Research, 43*, D204-D212

Tamura, K., Peterson, D., Peterson, N., Stecher, G., Nei, M., & Kumar, S. (2011) MEGA5: Molecular evolutionary genetics analysis using maximum likelihood, evolutionary distance, and maximum parsimony methods. *Molecular Biology and Evolution, 28*(10), 2731-2739

Thorburn, A. N., Macia, L., & Mackay, C. R. (2014) Diet, metabolites, and "western-lifestyle" inflammatory diseases. *Immunity, 40*(6), 833-842

Tohka, S., Laukkanen, M., Jalkanen, S., & Salmi, M. (2001) Vascular adhesion protein 1 (VAP-1) functions as a molecular brake during granulocyte rolling and mediates recruitment in vivo. *FASEB Journal, 15*(2), 373-382

Vainio, P. J., Kortekangas-Savolainen, O., Mikkola, J. H., Jaakkola, K., Kalimo, K., Jalkanen, S., & Veromaa, T. (2005) Safety of blocking vascular adhesion protein-1 in patients with contact dermatitis. *Basic & Clinical Pharmacology & Toxicology, 96*(6), 429-435

Varis, A., Wolf, M., Monni, O., Vakkari, M. L., Kokkola, A., Moskaluk, C., Frierson, H., Powell, S. M., Knuutila, S., Kallioniemi, A., & El-Rifai, W. (2002) Targets of gene amplification and overexpression at 17q in gastric cancer. *Cancer Research, 62*(9), 2625-2629

Wang, E. Y., Gao, H., Salter-Cid, L., Zhang, J., Huang, L., Podar, E. M., Miller, A., Zhao, J., O'rourke, A., Linnik, M. D. (2006) Design, synthesis, and biological evaluation of semicarbazide-sensitive amine oxidase (SSAO) inhibitors with anti-inflammatory activity. *Journal of Medicinal Chemistry, 49*(7), 2166-2173

Weston, C. J., Shepherd, E. L., Claridge, L. C., Rantakari, P., Curbishley, S. M., Tomlinson, J. W., Huscher, S. G., Reynolds, G. M., Aalto, K., Anstee, Q. M., Jalkanen, S., Salmi, M., Smith, D. J., Day, C. P., & Adams, D. H. (2015) Vascular adhesion protein-1 promotes liver inflammation and drives hepatic fibrosis. *The Journal of Clinical Investigation, 125*(2), 501-520

Wilmot, C. M., Hajdu, J., McPherson, M. J., Knowles, P. F., & Phillips, S. E. (1999) Visualization of dioxygen bound to copper during enzyme catalysis. *Science, 286*(5445), 1724-1728

Wilmot, C. M., Murray, J. M., Alton, G., Parsons, M. R., Convery, M. A., Blakeley, V., Corner, A. S., Palcic, M. M., Knowles, P. F., McPherson, M. J., & Phillips, S. E. (1997) Catalytic mechanism of the quinoenzyme amine oxidase from escherichia coli: Exploring the reductive half-reaction. *Biochemistry, 36*(7), 1608-1620

Yanaba, K., Yoshizaki, A., Muroi, E., Ogawa, F., Shimizu, K., & Sato, S. (2013) Increased circulating soluble vascular adhesion protein-1 levels in systemic sclerosis: Association with lower frequency and severity of interstitial lung disease. *International Journal of Rheumatic Diseases, 16*(4), 442-447

Yegutkin, G. G., Salminen, T., Koskinen, K., Kurtis, C., McPherson, M. J., Jalkanen, S., & Salmi, M. (2004) A peptide inhibitor of vascular adhesion protein-1 (VAP-1) blocks leukocyte-endothelium interactions under shear stress. *European Journal of Immunology, 34*(8), 2276-2285

Yoong, K. F., McNab, G., Hubscher, S. G., & Adams, D. H. (1998) Vascular adhesion protein-1 and ICAM-1 support the adhesion of tumor-infiltrating lymphocytes to

tumor endothelium in human hepatocellular carcinoma. *Journal of Immunology, 160*(8), 3978-3988

Zhang, Q., Mashima, Y., Noda, S., Imamura, Y., Kudoh, J., Shimizu, N., Nishiyama, T., Umeda, S., Oguchi, Y., Tanaka, Y., & Iwata, T. (2003) Characterization of AOC2 gene encoding a copper-binding amine oxidase expressed specifically in retina. *Gene, 318*, 45-53

Zorzano A., Abella A., Marti L., Carpene C., Palacin M. och Testar X. 2003. Semicarbazide-sensitive amino oxidase activity exerts insulin-like effects on glucose metabolism and insulin-signaling pathways in adipose cells. *Biochim Biophys Acta* 1647(1-2), 3-9